

## ORIGINAL ARTICLE

# Human-engineered Treg-like cells suppress FOXP3-deficient T cells but preserve adaptive immune responses *in vivo*

Yohei Sato<sup>1</sup> , Laura Passerini<sup>2</sup>, Brian D Piening<sup>3</sup>, Molly Javier Uyeda<sup>1,4</sup>, Marianne Goodwin<sup>1</sup>, Silvia Gregori<sup>2</sup>, Michael P Snyder<sup>5</sup>, Alice Bertaina<sup>1</sup>, Maria-Grazia Roncarolo<sup>1,4,6†</sup> & Rosa Bacchetta<sup>1,6†</sup><sup>1</sup>Department of Pediatrics, Division of Hematology, Oncology, Stem Cell Transplantation and Regenerative Medicine, Stanford University School of Medicine, Stanford, CA, USA<sup>2</sup>Mechanisms of Peripheral Tolerance Unit, San Raffaele Telethon Institute for Gene Therapy (SR-TIGET), IRCCS San Raffaele Scientific Institute, Milan, Italy<sup>3</sup>Earle A Chiles Research Institute, Providence Portland Medical Center, Portland, OR, USA<sup>4</sup>Institute for Stem Cell Biology and Regenerative Medicine, Stanford University School of Medicine, Stanford, CA, USA<sup>5</sup>Department of Genetics, Stanford University School of Medicine, Stanford, CA, USA<sup>6</sup>Center for Definitive and Curative Medicine (CDCM), Stanford University School of Medicine, Stanford, CA, USA**Correspondence**R Bacchetta, Stanford University, Lorry I. Lokey Stem Cell Research Building, 265 Campus Drive West, Room 3039, Stanford, CA 94305, USA.  
E-mail: rosab@stanford.edu

†Equal contributors.

Received 1 May 2020;

Revised 12 August and 24 October 2020;

Accepted 25 October 2020

doi: 10.1002/cti2.1214

*Clinical & Translational Immunology*  
2020; 9: e1214**Abstract**

**Objectives.** Genetic or acquired defects in FOXP3<sup>+</sup> regulatory T cells (Tregs) play a key role in many immune-mediated diseases including immune dysregulation polyendocrinopathy, enteropathy, X-linked (IPEX) syndrome. Previously, we demonstrated CD4<sup>+</sup> T cells from healthy donors and IPEX patients can be converted into functional Treg-like cells by lentiviral transfer of FOXP3 (CD4<sup>LVFOXP3</sup>). These CD4<sup>LVFOXP3</sup> cells have potent regulatory function, suggesting their potential as an innovative therapeutic. Here, we present molecular and preclinical *in vivo* data supporting CD4<sup>LVFOXP3</sup> cell clinical progression. **Methods.** The molecular characterisation of CD4<sup>LVFOXP3</sup> cells included flow cytometry, qPCR, RNA-seq and TCR-seq. The *in vivo* suppressive function of CD4<sup>LVFOXP3</sup> cells was assessed in xenograft-versus-host disease (xeno-GvHD) and FOXP3-deficient IPEX-like humanised mouse models. The safety of CD4<sup>LVFOXP3</sup> cells was evaluated using peripheral blood (PB) humanised (hu)- mice testing their impact on immune response against pathogens, and immune surveillance against tumor antigens. **Results.** We demonstrate that the conversion of CD4<sup>+</sup> T cells to CD4<sup>LVFOXP3</sup> cells leads to specific transcriptional changes as compared to CD4<sup>+</sup> T-cell transduction in the absence of FOXP3, including upregulation of Treg-related genes. Furthermore, we observe specific preservation of a polyclonal TCR repertoire during *in vitro* cell production. Both allogeneic and autologous CD4<sup>LVFOXP3</sup> cells protect from xeno-GvHD after two sequential infusions of effector T cells. CD4<sup>LVFOXP3</sup> cells prevent hyper-proliferation of CD4<sup>+</sup> memory T cells in the FOXP3-deficient IPEX-like hu-mice. CD4<sup>LVFOXP3</sup> cells do not impede *in vivo* expansion of antigen-primed T cells or tumor clearance in the PB hu-mice. **Conclusion.** These data support the clinical readiness of CD4<sup>LVFOXP3</sup> cells to treat IPEX syndrome and other

immune-mediated diseases caused by insufficient or dysfunctional FOXP3<sup>+</sup> Tregs.

**Keywords:** CRISPR/Cas9, FOXP3, gene therapy, IPEX syndrome, lentiviral vector, regulatory T cells

## INTRODUCTION

Regulatory T cells (Tregs) are CD4<sup>+</sup>CD25<sup>+</sup> T cells that maintain tolerance to self-antigens and non-harmful foreign antigens.<sup>1,2</sup> FOXP3 is a critical transcription factor for Treg function in both mice and human.<sup>3,4</sup> Because Tregs exhibit potent immunosuppressive function, Treg immunotherapies using *ex vivo* isolated or *in vitro* expanded Tregs have been used in the clinic for several diseases, including graft-versus-host disease (GvHD) after allogeneic hematopoietic stem cell transplantation (HSCT)<sup>5</sup> and early-onset type 1 diabetes (T1D).<sup>6</sup> Although the completed clinical trials have proven that Tregs can be safely administered, Treg cell therapies still present several challenges including obtaining enough Treg product for treatment, Treg survival and stability *in vivo* and long-term efficacy.<sup>7</sup>

The key role of Tregs in maintaining tolerance is exemplified by loss-of-function *FOXP3* mutations resulting in primary Treg dysfunction, leading to the severe autoimmune disease, immune dysregulation, polyendocrinopathy, enteropathy, X-linked (IPEX) syndrome.<sup>8</sup> Current therapies for IPEX syndrome are immunosuppression and/or HSCT. However, both therapeutic options have side effects, limited efficacy and often unfavorable long-term prognosis.<sup>9</sup> Thus, the IPEX syndrome represents a high unmet medical need.

To find novel strategies that overcome current Treg cell therapy limitations for autoimmune diseases, including IPEX syndrome, allergies and allograft rejection, we have pursued *FOXP3* gene transfer to generate Tregs *in vitro*. We previously demonstrated that Treg-like cells can be engineered using lentiviral transduction of *FOXP3* (LV-FOXP3) in CD4<sup>+</sup> T cells (CD4<sup>LVFOXP3</sup> cells).<sup>10</sup> In addition, we showed that lentiviral *FOXP3* gene transfer can successfully convert IPEX patient-derived CD4<sup>+</sup> effector T cells (Teffs) into Treg-like cells, thus confirming that the expression of mutant FOXP3 from the genomic loci in IPEX patient Teffs does not interfere with the Treg conversion process.<sup>11</sup>

In the present work, we determine the gene expression profile and TCR repertoire of *in vitro* generated CD4<sup>LVFOXP3</sup> cells. We demonstrate that CD4<sup>LVFOXP3</sup> cells show functional overlap with CD4<sup>+</sup>CD25<sup>+</sup>FOXP3<sup>+</sup> Tregs, and specific transcriptional changes not observed in control CD4<sup>LVNGFR</sup> cells, including upregulation of known Treg-related genes. In addition, CD4<sup>LVFOXP3</sup> cells show a polyclonal TCR repertoire, indicating that, during *in vitro* manipulation, the *FOXP3* gene transfer in Teffs does not alter the TCR repertoire. Moreover, we show that CD4<sup>LVFOXP3</sup> cells have strong *in vivo* regulatory potency and that autologous and allogeneic CD4<sup>LVFOXP3</sup> cells are equivalent in suppressing activated Teffs from healthy donors. Importantly, we demonstrate that CD4<sup>LVFOXP3</sup> cells can suppress FOXP3-deficient cells in a novel IPEX-like humanised mouse model (hu-mouse), generated by reconstituting NSG mice with human hematopoietic stem and progenitor cells genetically deleted for *FOXP3* using CRISPR-Cas9. Finally, polyclonal CD4<sup>LVFOXP3</sup> cells do not hinder host immunity against various pathogens including fungal and viral antigens in a hu-mouse model. Similarly, CD4<sup>LVFOXP3</sup> cells do not prevent tumor immunity in a skin sarcoma model.

Overall, these data show that human-engineered CD4<sup>LVFOXP3</sup> cells suppress FOXP3-deficient T cells but preserve adaptive immune responses *in vivo*, providing a strong rationale for their application in autoimmune and immune regulatory disorders, including severe monogenic paediatric diseases, such as IPEX syndrome.

## RESULTS

### CD4<sup>LVFOXP3</sup> cells acquire a Treg-like phenotype and function *in vitro*

We generated CD4<sup>LVFOXP3</sup> cells from either healthy donors or IPEX patients, using an LV vector (LV-FOXP3) that was modified from our original construct (pCCL-FOXP3)<sup>10</sup> to make it suitable for clinical-grade use. Both the original pCCL-FOXP3 and modified LV-FOXP3 vectors contain the

truncated nerve growth factor receptor (*NGFR*) as a surface marker gene. Transduction efficiency and vector copy number (VCN) in the CD4<sup>LVFOXP3</sup> cells generated with LV-FOXP3 (pCCL-FOXP3 modified) were comparable to those described in transduced cells obtained with the original vector<sup>10,11</sup> (see Methods and Supplementary figure 1a).

Both healthy donor and IPEX CD4<sup>LVFOXP3</sup> cells were consistently CD25<sup>high</sup> CD127<sup>low</sup> FOXP3<sup>positive</sup>, a phenotypic hallmark of naturally occurring Tregs (Figure 1a and b). Furthermore, the combined analysis of CD4<sup>LVFOXP3</sup> cells generated from both healthy donors and IPEX patients demonstrated that the CD25 expression (%) was significantly higher when compared to that observed in CD4<sup>UT</sup> cells ( $P$ -value = 0.0043). In agreement with our previous findings, CD4<sup>LVFOXP3</sup> cells generated from two new IPEX patients, GD0037 and GD0064, had a Treg-like phenotype that was similar to the CD4<sup>LVFOXP3</sup> cells generated from healthy donors. This finding was despite the fact that patient GD0037 had been exposed to long-term immunosuppression and his T cells have residual expression of mutant FOXP3, while T cells from patient GD0064 were harvested at disease onset and had no FOXP3 expression.<sup>12</sup> These results further prove that LV-mediated Treg-like 'conversion' can be achieved in cells completely lacking FOXP3 expression, as well as T cells from patients being treated with ongoing immune suppression.

In addition to the hallmark Treg markers listed above, we found that CD4<sup>LVFOXP3</sup> cells express other Treg-related proteins (CTLA-4, ICOS, GITR, IL-1R1 and IL-6R,  $P$ -values = 0.0087, 0.0022, 0.0022, 0.0022 and 0.0260) and co-inhibitory molecules (TIGIT and TIM-3,  $P$ -values = 0.0152 and 0.0043). The expression of these genes was significantly increased in CD4<sup>LVFOXP3</sup> cells as compared to control cells transduced with *NGFR* alone, CD4<sup>LVNGFR</sup> cells (Figure 1c). We observed no significant difference in PD-1, HELIOS and LAG3 expression. CD226 was the only protein that was significantly decreased in CD4<sup>LVFOXP3</sup> cells relative to controls ( $P$  = 0.0087). The expression of mRNA for other selected Treg-related markers (*FOXP3*, *LGMM*, *EOS*, *IL-12A* and *EBI3*) was analysed by qPCR and is shown by both  $\Delta$ CT and relative expression (Figure 1d, Supplementary figure 1d) for freshly isolated Tregs, non-Tregs and activated Tregs included as controls. Consistent with the

protein levels determined by flow cytometry (FACS) analysis, CD4<sup>LVFOXP3</sup> cells had increased *FOXP3* and *NGFR* mRNA expression. The mRNAs for *EOS* and *EBI3* were also significantly increased in CD4<sup>LVFOXP3</sup> cells compared to control CD4<sup>LVNGFR</sup> cells. These data show that in addition to CD25<sup>high</sup> and CD127<sup>low</sup>, engineered Treg-like CD4<sup>LVFOXP3</sup> cells upregulate functionally relevant co-inhibitory molecules, Treg-related genes, transcription factors and cytokine receptors.

To understand whether *FOXP3* gene transfer impacts TCR repertoire diversity during the generation of CD4<sup>LVFOXP3</sup> cells *in vitro*, we compared the TCR repertoires from healthy donors and IPEX patients (GD0037 and GD0064) of (1) CD4<sup>+</sup> T cells prior to transduction and culturing, and (2) CD4<sup>LVFOXP3</sup> cells or control CD4<sup>LVNGFR</sup> cells after transduction and at the end of production. The healthy donors had polyclonal TCR repertoires in CD4<sup>+</sup> T cells, and this TCR diversity was maintained in CD4<sup>LVFOXP3</sup> cells and CD4<sup>LVNGFR</sup> cells (Mean clonality index: CD4<sup>+</sup> T cells 0.364, CD4<sup>LVFOXP3</sup> cells 0.353, CD4<sup>LVNGFR</sup> cells 0.359) (Figure 2a). Similarly, both GD0037 and GD0064 IPEX CD4<sup>+</sup> T cells had a polyclonal repertoire that was maintained *in vitro* after LV-mediated FOXP3 expression (Mean clonality index: GD0037: CD4<sup>+</sup> T cells 0.357, CD4<sup>LVFOXP3</sup> cells 0.358, CD4<sup>LVNGFR</sup> cells 0.340; and GD0064: CD4<sup>+</sup> T cells 0.299, CD4<sup>LVFOXP3</sup> cells 0.283, CD4<sup>LVNGFR</sup> cells 0.286; Figure 2b). CDR3 length diversity was comparable between healthy donors and IPEX patients. Polyclonal TCR V-beta usage was maintained in CD4<sup>LVFOXP3</sup> cells (and in control CD4<sup>LVNGFR</sup> cells) generated from both healthy donors and IPEX patients (Figure 2c). Overall, there was no significant difference in the TCR V-beta usage of CD4<sup>+</sup> T cells and the CD4<sup>LVFOXP3</sup> cells generated *in vitro*. These data indicate that CD4<sup>LVFOXP3</sup> cells maintain a polyclonal TCR repertoire.

Given that we are using an LV vector that was modified from our original construct, we validated that the Treg-like function of CD4<sup>LVFOXP3</sup> cells generated from both healthy donors and IPEX patients GD0037 and GD0064 was maintained, by analysing signature cytokine production, proliferative capacity and suppressive functions. We found that CD4<sup>LVFOXP3</sup> cells from healthy donors and both IPEX patients have reduced production of IL-2, IL-4 and interferon (IFN)- $\gamma$ , and similar production of IL-17A and IL-22, when compared to control untransduced CD4<sup>+</sup> T

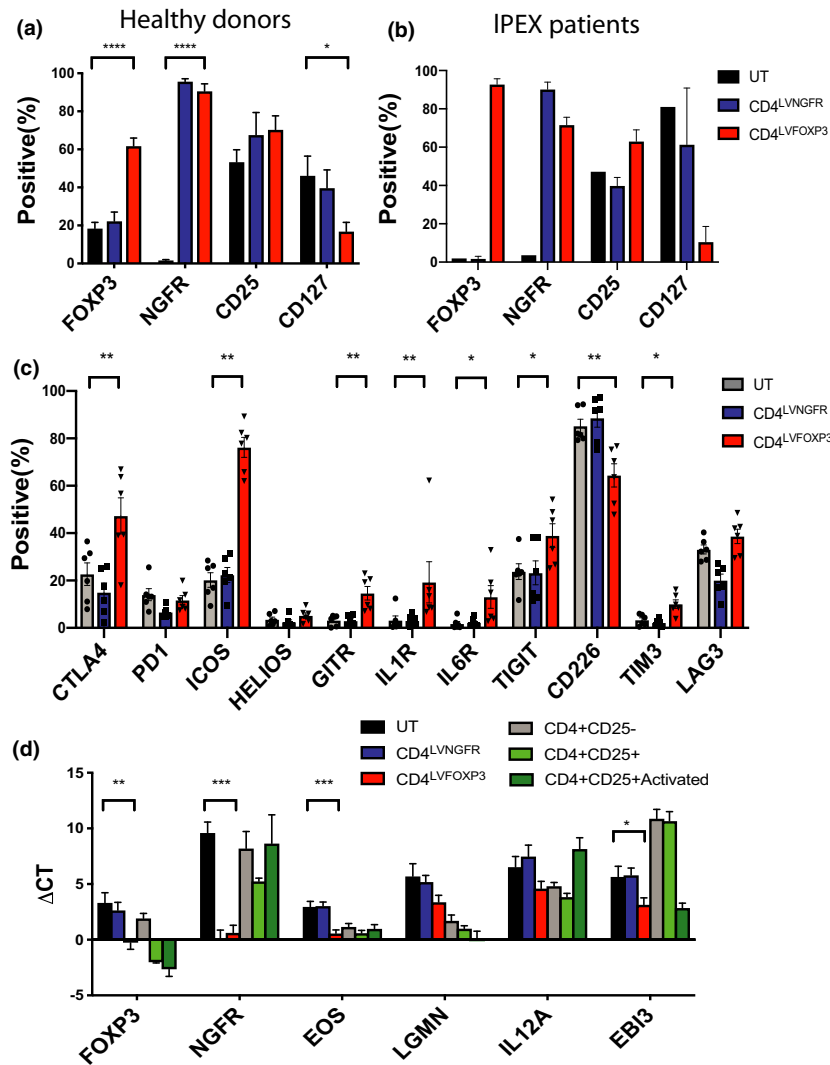


**Figure 1.** CD4<sup>LVFOXP3</sup> cells have a Treg-like phenotype. Expression of bona fide Treg molecules measured by FACS in (a) healthy donors ( $n = 8$ , mean + SEM) and (b) patients with IPEX syndrome ( $n = 2$ , mean + SEM). (c) Expression of other Treg-related molecules measured by FACS ( $n = 6$ , mean + SEM). (d) Expression of Treg-related molecules measured by real-time PCR. *HPRT* mRNA was used as internal control. Relative expression was calculated by  $\Delta CT$  ( $n = 8$ , mean + SEM). UT, untransduced CD4<sup>+</sup> T cells cultured in parallel with CD4<sup>LVFOXP3</sup> and CD4<sup>LVNGFR</sup> cells. *P*-values: \* < 0.05, \*\* < 0.01, \*\*\* < 0.001, \*\*\*\* < 0.0001.

cells (CD4<sup>UT</sup> cells) and CD4<sup>LVNGFR</sup> cells (Supplementary figure 2a and b, Supplementary tables 1 and 2).

We next analysed the proliferative capacity as it is considered another hallmark of Tregs. Compared to CD4<sup>UT</sup> and CD4<sup>LVNGFR</sup> control cells (CD4<sup>UT</sup> cells 45.5 ± 4.5% proliferation, CD4<sup>LVNGFR</sup> cells 45 ± 3.8% proliferation, mean ± SEM,  $n = 8$ ), healthy donor CD4<sup>LVFOXP3</sup> cells had significantly reduced proliferative capacity (CD4<sup>LVFOXP3</sup> cells 11.2 ± 1.0% proliferation, mean ± SEM,  $n = 8$ ,  $P = 0.0002$ ) (Supplementary figure 2c). CD4<sup>LVFOXP3</sup> cells generated from IPEX

patients GD0037 and GD0064 also had reduced proliferative capacity (CD4<sup>LVFOXP3</sup> cells 30.5 ± 0.2% proliferation, mean ± SEM,  $n = 2$ ) compared to CD4<sup>UT</sup> and CD4<sup>LVNGFR</sup> cells from the same patients (CD4<sup>UT</sup> cells 57.3 ± 1.65% proliferation, CD4<sup>LVNGFR</sup> cells 59.2 ± 0.5% proliferation, mean ± SEM,  $n = 2$ ; Supplementary figure 2d).

Finally, we determined the *in vitro* suppressive function of CD4<sup>LVFOXP3</sup> cells from healthy donors, or GD0037 and GD0064 IPEX patients. Healthy donor CD4<sup>LVFOXP3</sup> cells suppressed the proliferation of responder cells in a dose-

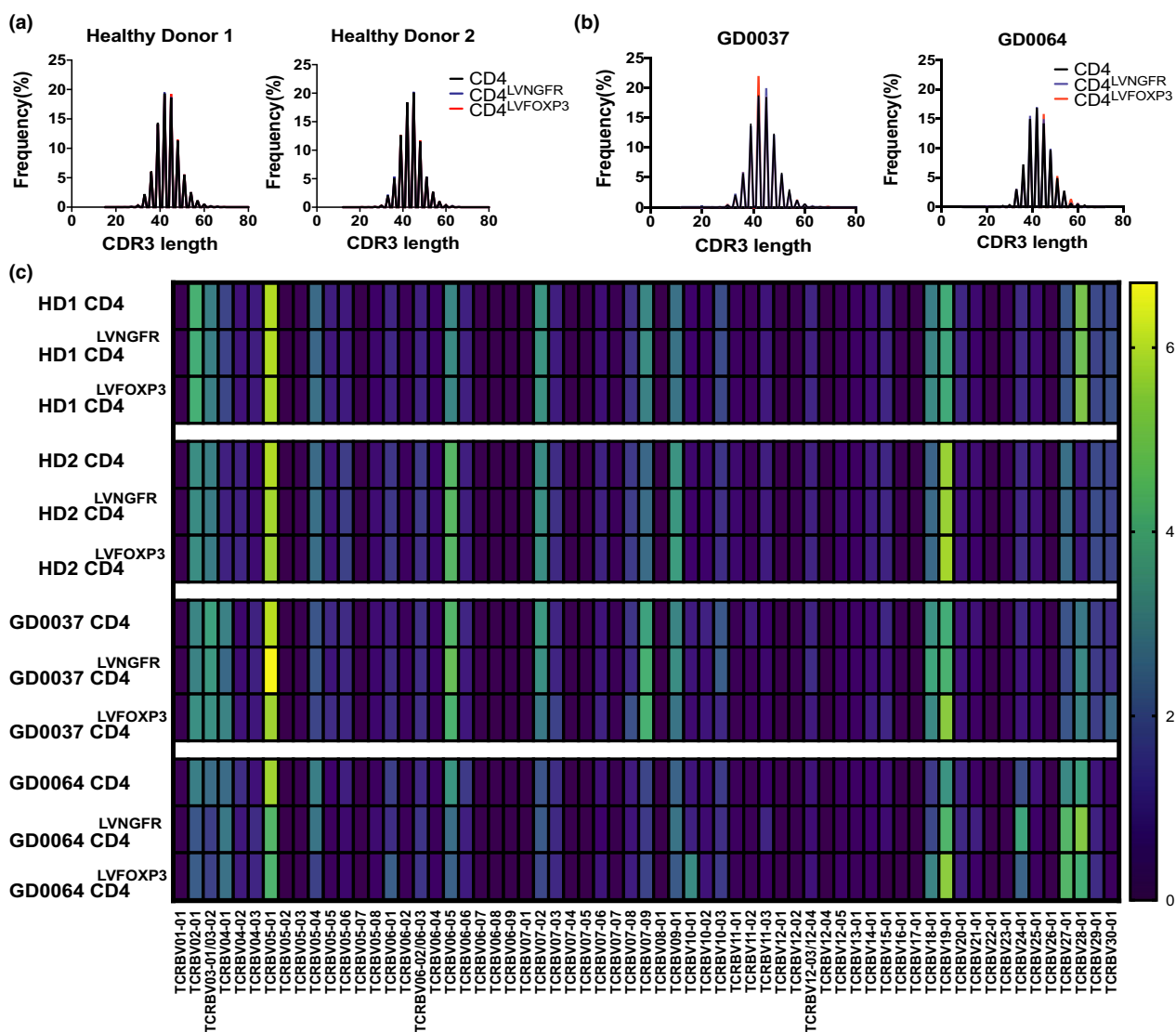


**Figure 2.** CD4<sup>LVFOXP3</sup> cells maintain a polyclonal TCR repertoire. CDR3 length of CD4<sup>+</sup> T cells (prior to the culture), CD4<sup>LVNGFR</sup> and CD4<sup>LVFOXP3</sup> cells from (a) healthy donors ( $n = 2$ ) and (b) IPEX patients ( $n = 2$ ). (c) TCRβ usage of CD4<sup>+</sup> T cells, CD4<sup>LVNGFR</sup> and CD4<sup>LVFOXP3</sup> cells from the same healthy donors ( $n = 2$ ) and IPEX patients ( $n = 2$ ). HD = healthy donors, GD0037 and GD0064 = IPEX patients.

dependent manner (R:S = 1:1, Suppression index  $86.2 \pm 5.7$ , mean  $\pm$  SEM,  $n = 8$ ,  $P = 0.0016$ ). Inhibition of proliferation was significantly higher than CD4<sup>LVNGFR</sup> cells (R:S = 1:1, Suppression index  $24.6 \pm 9.2$ , mean  $\pm$  SEM,  $n = 8$ ; Supplementary figure 2e). CD4<sup>LVFOXP3</sup> cells generated from IPEX patients also suppressed Teff proliferation in a dose-dependent fashion (R:S = 1:1, Suppression index  $63.9 \pm 1.9$ , mean  $\pm$  SEM,  $n = 3$ ,  $P = 0.0120$ ; Supplementary figure 2f).

Collectively, these phenotypic and functional data indicate that the modified LV vector maintains CD4<sup>LVFOXP3</sup> Treg-like identity and

function for both healthy donor and IPEX patient cells.

### CD4<sup>LVFOXP3</sup> cells have a Treg-like transcription profile

As CD4<sup>LVFOXP3</sup> cells originate from Teffs and acquire the phenotypic and functional characteristics of Tregs, we investigated how constitutive FOXP3 expression affected the Teff gene profile. We compared the transcriptomes of CD4<sup>LVFOXP3</sup> cells, freshly isolated Tregs (CD25<sup>+</sup>CD127<sup>-</sup>) and non-Tregs (CD4<sup>+</sup>CD25<sup>-</sup>), all

derived from the same donor and generated in parallel ( $n = 3$ ). Control cells (CD4<sup>LVNGFR</sup> cells) transduced with vector expressing only *NGFR* were also generated in parallel ( $n = 3$ ). Principal component analysis (PCA) and hierarchical clustering showed that both CD4<sup>LVFOXP3</sup> and CD4<sup>LVNGFR</sup> cells have similar gene expression patterns and are quite divergent from freshly isolated Tregs and non-Tregs from the same donor (Figure 3a and b). These data indicate that *in vitro* transduced Teffs maintain their lineage features. CD4<sup>LVFOXP3</sup> and CD4<sup>LVNGFR</sup> cells were overall transcriptionally similar (Supplementary figure 3b), but when compared to CD4<sup>LVNGFR</sup> cells, CD4<sup>LVFOXP3</sup> cells showed 41 differentially expressed genes (DEGs) that were enriched for known Treg-related genes (31 upregulated, 10 downregulated, false discovery rate FDR < 0.05; Figure 3c, Supplementary table 3). In addition, despite substantial differences between the gene expression profiles of CD4<sup>LVFOXP3</sup> cells and freshly isolated Tregs, CD4<sup>LVFOXP3</sup> cells have a transcriptome that is more similar to that of Tregs than non-Tregs (Supplementary figure 3c). As expected, freshly isolated Tregs have a unique gene expression profile compared to non-Tregs (Supplementary figure 3a) with 413 differentially expressed genes (DEGs, 251 upregulated, 162 downregulated, FDR < 0.05) compared to the non-Tregs (Supplementary table 4).

To identify shared genes between freshly isolated Tregs and CD4<sup>LVFOXP3</sup> cells, we directly compared DEGs (FDR < 0.05) in these two cell populations and found seven genes upregulated in both cell types and that were also among the 31 upregulated genes found in CD4<sup>LVFOXP3</sup> cells but not in CD4<sup>LVNGFR</sup> cells (Figure 3d). These genes are known Treg-associated genes, *FOXP3*, *CTLA4* and *IL1R1*, as well as *F5* (described in human Tregs but not yet associated with suppressive function<sup>13</sup>), *MEOX1* (described in epigenetic signature of human Tregs<sup>14</sup>), and *TJP3* and *TBC1D4* (only reported in mouse Tregs<sup>15,16</sup>; Figure 3e). There were no shared genes among the downregulated genes in Tregs and CD4<sup>LVFOXP3</sup> cells using the above FDR cut-off (Figure 3f). These data show that stable FOXP3 expression in Teffs induces specific transcriptional changes, including upregulation of few Treg-related genes, suggesting that they could be responsible for the acquisition of the phenotype and suppressive function by CD4<sup>LVFOXP3</sup> cells.

### Autologous CD4<sup>LVFOXP3</sup> cells are suppressive in a xeno-GvHD mouse model

Tregs have largely been used in an allogeneic setting to suppress the proliferation of responding Teffs.<sup>17</sup> In view of the potential use of CD4<sup>LVFOXP3</sup> cells in autoimmune diseases, we tested the *in vivo* efficacy of autologous vs allogeneic CD4<sup>LVFOXP3</sup> cells in a xeno-GvHD mouse model.<sup>18–20</sup> Both allogeneic and autologous CD4<sup>LVFOXP3</sup> cells co-injected with Teffs were equally effective at improving the survival of xeno-GvHD mice when compared to the Teff-alone control (Figure 4a). Weight loss because of xeno-GvHD progression was also alleviated by co-injection of either allogeneic or autologous CD4<sup>LVFOXP3</sup> cells (Figure 4b). Peripheral engraftment of Teff responders was similarly suppressed by either allogeneic or autologous CD4<sup>LVFOXP3</sup> cells (Figure 4c). Notably, NGFR<sup>+</sup> T cells (a marker for CD4<sup>LVFOXP3</sup> cells) were detected in the peripheral blood up to week 3 post-injection with autologous CD4<sup>LVFOXP3</sup> cells, which was longer survival than that observed for allogeneic CD4<sup>LVFOXP3</sup> cells (Figure 4d).

The phenotype of the remaining Teffs in the spleen was analysed 2–3 weeks after injection. There was no significant difference in the frequency of Teffs in each condition (Figure 4e). Co-injection of either allogeneic or autologous CD4<sup>LVFOXP3</sup> cells resulted in a significant reduction in activation markers including CD69, CD71 and HLA-DR in Teffs, while Teff CD25 expression was reduced in the presence of either CD4<sup>LVFOXP3</sup> or CD4<sup>LVNGFR</sup> cells (Figure 4f). Thus, co-infusion of either allogeneic or autologous CD4<sup>LVFOXP3</sup> cells did not affect the total proportion of Teffs in the spleen, although their overall activation state in the spleen was clearly reduced.

Overall, both allogeneic and autologous CD4<sup>LVFOXP3</sup> cells extend the survival and diminish the severity of xeno-GvHD reactions. We observed a survival advantage of autologous CD4<sup>LVFOXP3</sup> cells compared to allogeneic CD4<sup>LVFOXP3</sup> cells, most likely because of the absence of responder cell alloreactivity.

To assess whether mice injected with autologous CD4<sup>LVFOXP3</sup> cells remain tolerant, the xeno-GvHD mice were re-challenged with the same responding Teffs ( $2 \times 10^6$  cells) 2 weeks after the initial co-injection of autologous CD4<sup>LVFOXP3</sup> cells (re-challenge condition). Both Teffs alone

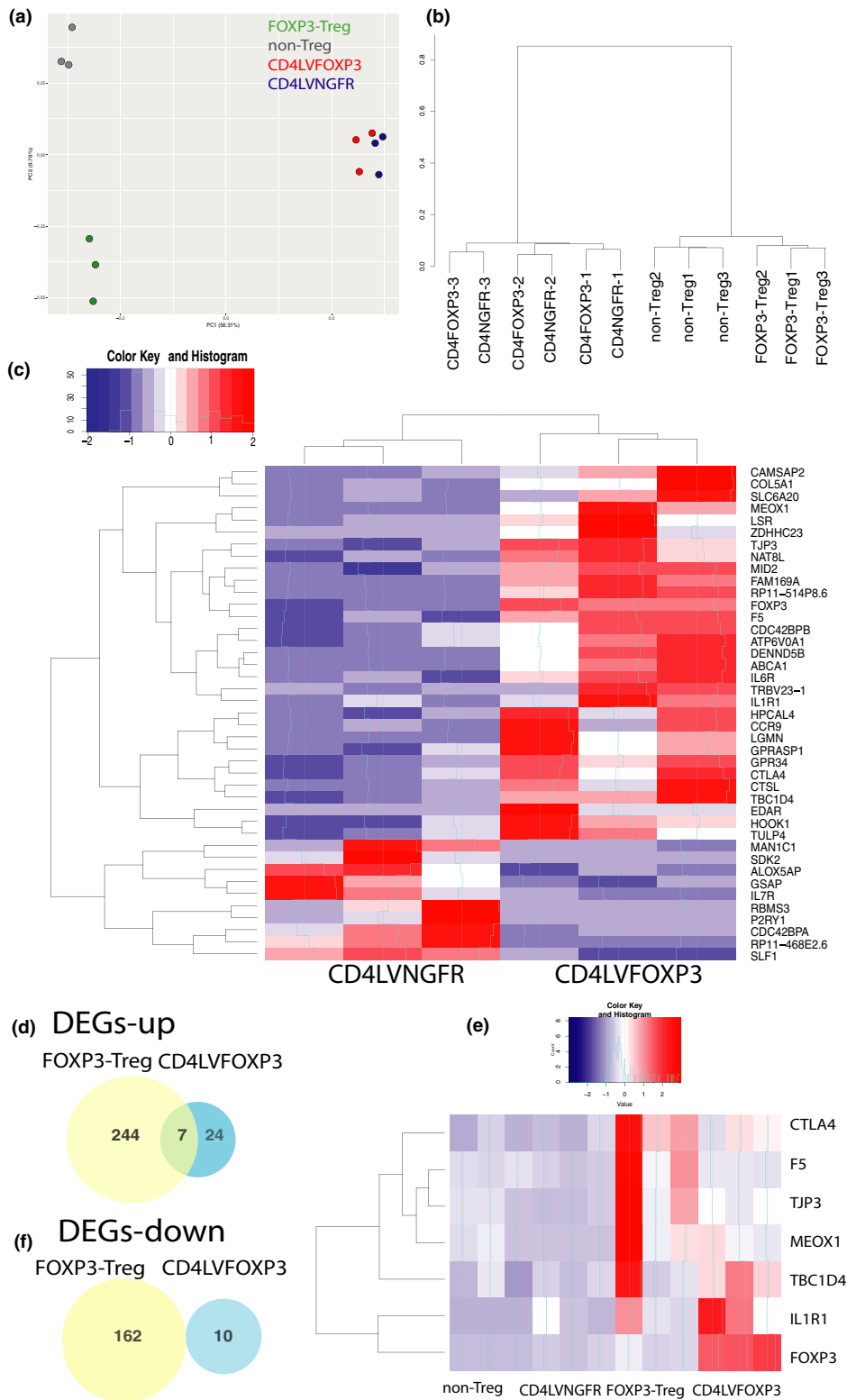


**Figure 3.** CD4<sup>LVFOXP3</sup> cells have a Treg-like gene expression profile. **(a)** Principal component analysis (PCA), **(b)** hierarchical cluster analysis (HCA), **(c)** heat map of differentially expressed genes (DEGs) between CD4<sup>LVFOXP3</sup> and CD4<sup>LVNGFR</sup> cells ( $n = 3$ ), **(d)** shared DEGs (upregulated) between freshly isolated FOXP3 Tregs and CD4<sup>LVFOXP3</sup> cells of the same donors. **(e)** Heat map of the seven shared upregulated genes between freshly isolated FOXP3 Tregs and CD4<sup>LVFOXP3</sup> cells. **(f)** DEGs (downregulated) in freshly isolated FOXP3 Tregs and CD4<sup>LVFOXP3</sup> cells.

and CD4<sup>LVNGFR</sup> cell co-injection conditions had already developed xeno-GvHD and thus were not re-challenged with the same Teffs. Control mice in which we injected Teffs 2 weeks after sublethal irradiation were tested in parallel (Teff-late condition).

Results showed that mice previously (at day 0) injected with autologous CD4<sup>LVFOXP3</sup> cells were resistant to re-challenge after a second injection of the same Teff (Figure 5a). Injection of Teffs at 2 weeks after sublethal irradiation caused a milder xeno-GvHD; however, the co-injection of CD4<sup>LVFOXP3</sup> cells provided significant protection against Teff-mediated xeno-GvHD. Minimal weight loss was observed after re-challenge, but it was less than that observed with Teffs alone, or after CD4<sup>LVNGFR</sup> cell co-injection (Figure 5b). Although the proliferation of Teffs was strongly suppressed by CD4<sup>LVFOXP3</sup> cell co-injection in the re-challenged mice, we did observe an increase in Teffs during the entire observational period (Figure 5c). The transduced cells survived *in vivo* up to week 3, and there was no additional survival advantage of transduced cells after the second injection (Figure 5d). These data suggest that CD4<sup>LVFOXP3</sup> cell injection induced a state of tolerance and/or resistance to subsequent re-challenge with Teffs.

### CD4<sup>LVFOXP3</sup> cells are suppressive in a *FOXP3* knockout hu-mouse model

One important question for clinical application of the CD4<sup>LVFOXP3</sup> cells is whether they are effective in conditions where immune regulation has been altered and the immune system activated. For example, IPEX patients display increased lymphoproliferation, especially in the CD4<sup>+</sup> memory T-cell compartment. To address this question, we generated a *FOXP3* knockout (KO) hu-mouse (*FOXP3* KO hu-mouse). We used CRISPR/Cas9 coupled with sgRNA targeting the *FOXP3* gene to edit human umbilical cord blood-derived CD34<sup>+</sup> hematopoietic stem and progenitor cells (HSPCs), and then transplanted these edited HSPCs into neonatal NSG mice. By flow cytometry, we detected peripheral blood (PB) engraftment between week 8 and week 10 and spleen engraftment at week 16 (Supplementary figure 4a). Average insertion and deletion (INDEL) frequency in edited HSPCs measured by TIDE analysis 3–5 days after editing was  $31.1 \pm 3.1\%$  (mean  $\pm$  SEM,  $n = 7$ ; Supplementary figure 4b).

The frequency of human (h) CD45<sup>+</sup> cells and CD8<sup>+</sup> T cells in PB was stable for 16 weeks and similar to that of mice injected with the unmodified HSPCs. In contrast, the frequency of CD4<sup>+</sup> T cells in the *FOXP3* KO hu-mice continued to increase (Supplementary figure 4c). The frequency of human (h) CD45<sup>+</sup> cells in PB (Supplementary figure 4d) and spleen (Supplementary figure 4e) was slightly higher in *FOXP3* KO hu-mice at week 16, but there was no statistically significant difference. The frequencies of CD4<sup>+</sup> (PB and spleen) and CD8<sup>+</sup> T cells (only spleen) were significantly increased in the *FOXP3* KO hu-mice. This increase was more apparent for the CD4<sup>+</sup> population. The CD4/CD8 ratio also was significantly increased in the *FOXP3* KO hu-mice in both PB ( $P$ -value = 0.0426) and spleen ( $P$ -value = 0.0200). This indicates that *FOXP3* KO hu-mice developed CD4<sup>+</sup> T-cell dominant lymphoproliferation, thus mimicking the lymphoproliferative phenotype found in IPEX patients.<sup>9</sup>

Control and *FOXP3* KO hu-mice both exhibited multilineage engraftment (Supplementary figure 5a). To specifically delineate where the increase in CD3<sup>+</sup> cells originated, we quantified different memory and naïve subpopulations within CD4<sup>+</sup> and CD8<sup>+</sup> T cells in the PB and spleen at week 16 (Supplementary figure 5b). The frequency of naïve CD4<sup>+</sup> T cells was significantly reduced in *FOXP3* KO mice in both PB (Supplementary figure 5c) and spleen (Supplementary figure 5d) when compared to unmodified hu-mice, while the CD8<sup>+</sup> naïve cells were comparable. When we analysed the spleen from *FOXP3* KO hu-mice at week 16, we found no significant difference in the frequency of the CD25<sup>+</sup> CD127<sup>-</sup> population compared to control. In contrast, the frequency of the FOXP3<sup>hi</sup> CD25<sup>+</sup> CD127<sup>-</sup> population was significantly reduced (Supplementary figure 5e). Overall, mice reconstituted with *FOXP3* KO HSPC had a CD4<sup>+</sup> T-cell dominant lymphoproliferation and a defect in Treg development, resembling IPEX patients.

Another characteristic of IPEX is tissue infiltration of T cells, especially in the gut. We found infiltrating CD4<sup>+</sup> T cells in the colons of the *FOXP3* KO hu-mice but not in the unmodified hu-mice (Supplementary figure 6). These results suggest the *FOXP3* KO hu-mice have decreased functional Tregs and are therefore unable to suppress CD4<sup>+</sup> T-cell tissue infiltration, as observed in IPEX patients.

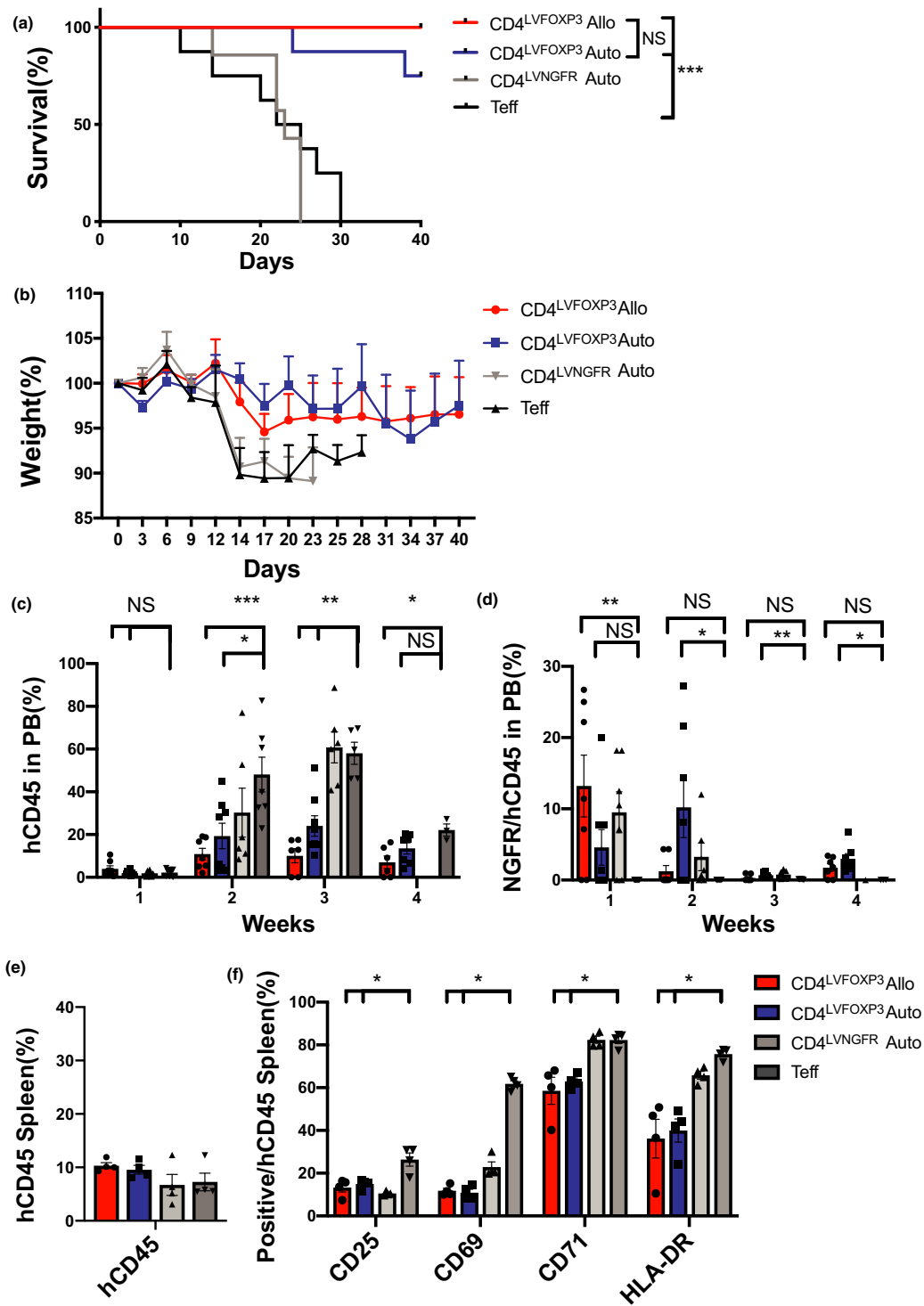


**Figure 4.** CD4<sup>LVFOXP3</sup> cells suppress xeno-GvHD in autologous condition. **(a)** Survival of xeno-GvHD mice with Teff alone or in the presence of CD4<sup>LVFOXP3</sup> cells (allogeneic or autologous) or autologous CD4<sup>LVNGFR</sup> cells ( $n = 7$  or  $8$ ). **(b)** Weight loss of xeno-GvHD mice under the same conditions ( $n = 7$  or  $8$ , mean  $\pm$  SEM). **(c)** Percentage of human (h) CD45<sup>+</sup> cells in peripheral blood (PB;  $n = 7$  or  $8$ , mean  $\pm$  SEM). **(d)** Percentage of NGFR<sup>+</sup> cells in hCD45<sup>+</sup> cells in PB of the mice ( $n = 7$  or  $8$ , mean  $\pm$  SEM). **(e)** Percentage of hCD45<sup>+</sup> cells in the spleen between weeks 2 and 3 ( $n = 4$ , mean  $\pm$  SEM). **(f)** Percentage of CD25, CD69, CD71 and HLA-DR-positive cells in hCD45<sup>+</sup> cells in the spleen between weeks 2 and 3 ( $n = 4$ , mean  $\pm$  SEM). Data are representative of two independently repeated experiments. All phenotyping was performed by FACS. *P*-values: \*  $< 0.05$ , \*\*  $< 0.01$ , \*\*\*  $< 0.001$ , \*\*\*\*  $< 0.0001$ .

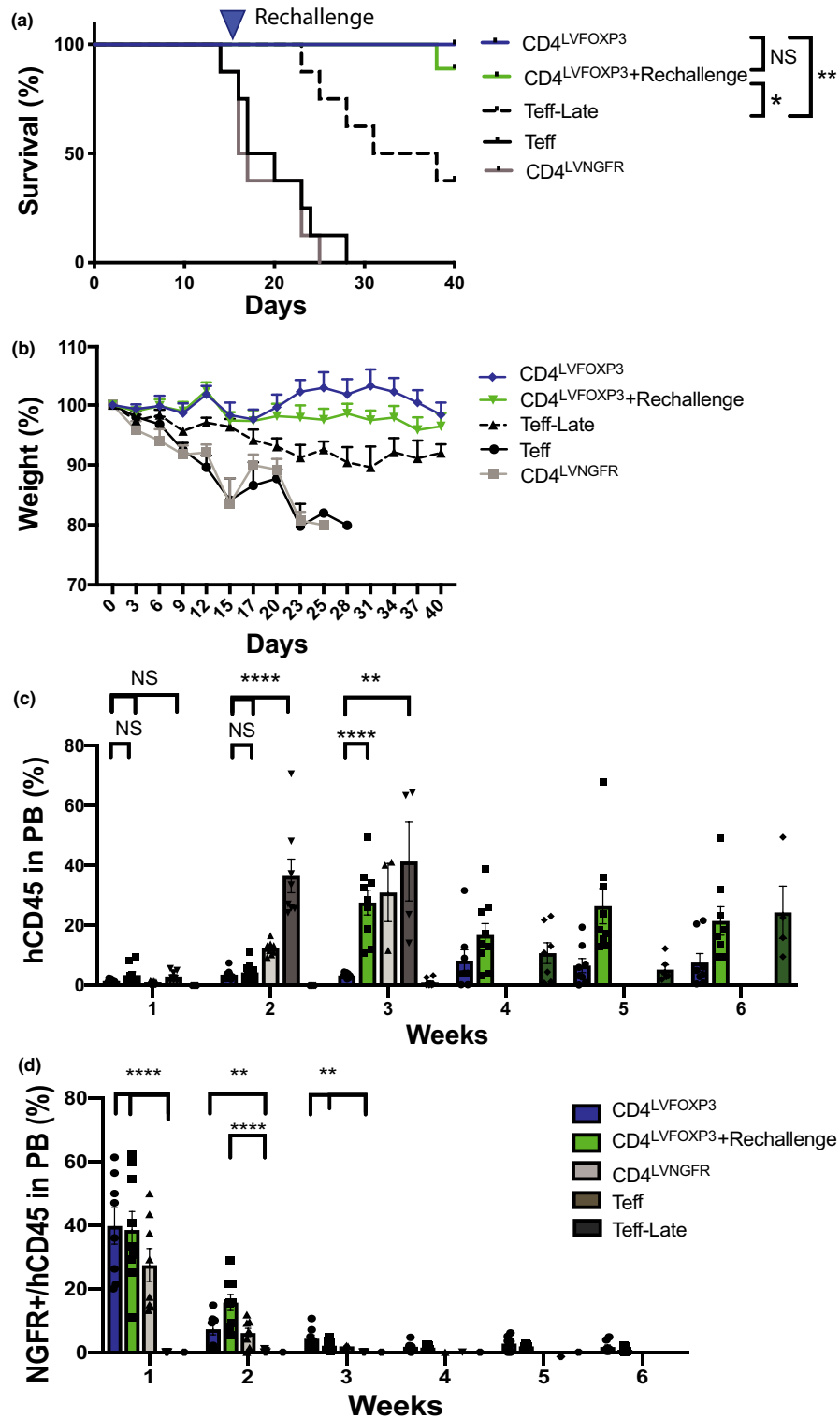


**Figure 5.** CD4<sup>LVFOXP3</sup> cells prevent xeno-GvHD reaction after re-challenge. **(a)** Survival of xeno-GvHD mice with Teff alone (day 0), Teff and CD4<sup>LVNGFR</sup>/CD4<sup>LVFOXP3</sup> cells co-injection (day 0), Teff-late (day 16) and re-challenge conditions (day 0 and day 16). Re-challenge mice received the same responding Teff (day 16) after the initial co-injection of autologous CD4<sup>LVFOXP3</sup> cells ( $n = 8$  or  $9$ ). **(b)** Weight loss of xeno-GvHD mice ( $n = 8$  or  $9$ , mean  $\pm$  SEM). **(c)** Percentage of human (h) CD45<sup>+</sup> cells in PB ( $n = 8$  or  $9$ , mean  $\pm$  SEM). **(d)** Percentage of NGFR<sup>+</sup> cells in hCD45<sup>+</sup> cells in PB ( $n = 8$  or  $9$ , mean  $\pm$  SEM). Data are representative of two independently repeated experiments. All phenotyping was performed by FACS. P-values: \*  $< 0.05$ , \*\*  $< 0.01$ , \*\*\*  $< 0.001$ , \*\*\*\*  $< 0.0001$ .

Next, we asked whether CD4<sup>LVFOXP3</sup> cells can suppress Teff lymphoproliferation in the *FOXP3* KO hu-mouse model, by injecting CD4<sup>LVFOXP3</sup> cells generated from the same HSPC donor at week 12, when the CD4<sup>+</sup> T cells started to increase. We observed significantly longer survival of *FOXP3* KO hu-mice after CD4<sup>LVFOXP3</sup> cell injection, compared to the *FOXP3* KO hu-mice not injected with CD4<sup>LVFOXP3</sup> cells (Figure 6a). The analysis of NGFR-positive cells (as a marker for CD4<sup>LVFOXP3</sup> cells) in the *FOXP3* KO hu-mice revealed that the percentage of peripheral CD4<sup>LVFOXP3</sup> cells decreased to almost undetectable at week 16 (i.e. 4 weeks after injection) (Figure 6b). Similarly, NGFR<sup>+</sup> cells were almost undetectable in the spleen at week 16.

Overall, human cell engraftment (CD3, CD13, CD19 and CD56) in both PB and spleen was not influenced by CD4<sup>LVFOXP3</sup> cell injection (Supplementary figure 7a). The increased CD4<sup>+</sup> T-cell frequency in the PB and spleen caused by lack of *FOXP3* was controlled by CD4<sup>LVFOXP3</sup> cell infusion. The frequency of CD8<sup>+</sup> T cells in the PB and spleen did not significantly increase after *FOXP3* KO, and it remained unchanged after CD4<sup>LVFOXP3</sup> cell injection. However, the increased CD4/CD8 ratio observed in the *FOXP3* KO hu-mice was alleviated by CD4<sup>LVFOXP3</sup> cell injection (Figure 6c and d). Next, we quantified the absolute number of hCD45<sup>+</sup>, CD4<sup>+</sup> and CD8<sup>+</sup> T cells in the spleen. The number of hCD45<sup>+</sup> cells in the spleen was significantly increased in *FOXP3* KO mice, an effect that was partially mitigated by CD4<sup>LVFOXP3</sup> cell injection. In contrast, the increase in the number of CD4<sup>+</sup> and CD8<sup>+</sup> T cells in the spleen was significantly diminished after CD4<sup>LVFOXP3</sup> cell injection (Figure 6e). INDEL frequency in PB was maintained 16 weeks after injection (Figure 6f).

The percentage of naïve cells out of CD4<sup>+</sup> and CD8<sup>+</sup> T cells and the infiltration of CD4<sup>+</sup> T cells in the colon were both improved after CD4<sup>LVFOXP3</sup> cell injection (Supplementary figure 7b–d; Supplementary figure 8). In summary, CD4<sup>LVFOXP3</sup> cells suppressed the CD4<sup>+</sup> T-cell dominant lymphoproliferation caused by *FOXP3* KO in the hu-mouse model without affecting overall human cell engraftment and other immune cells. These data strongly support that the *FOXP3* KO hu-mice are a suitable model to assess the efficacy of a Treg-replacement infusion with CD4<sup>LVFOXP3</sup> cells.

## Immunity against pathogens is preserved after CD4<sup>LVFOXP3</sup> cell administration

When compared to pharmacological immunosuppression, Treg cell therapy should provide the advantage of immune regulation while preserving immune responses to pathogens and immune surveillance against cancer. To test whether CD4<sup>LVFOXP3</sup> cells negatively affect immune responses against pathogens or cancer cells, we used hu-mouse models.<sup>21</sup> Briefly, NSG mice were humanised by co-injection of peripheral blood mononuclear cells (PBMCs) and mature dendritic cells (mDCs) that were previously pulsed *in vitro* with the fungal antigen, *Candida albicans* (candida). Either autologous CD4<sup>LVFOXP3</sup> or CD4<sup>LVNGFR</sup> cells derived from the same healthy donors were injected 6 days after PBMC injection, to allow initial engraftment of the Ag-primed responder cells (Figure 7a), but still be inhibitory in the xeno-GVHD model.<sup>11</sup> Donor PBMCs were preselected for positive immune responses against both tetanus toxoid and candida prior to injection. At the end of the *in vivo* experiment, the presence of IFN- $\gamma$ -positive cells in PBMCs was tested after restimulation *in vitro* with mDC pulsed with candida (Figure 7b). The frequency of antigen-specific IFN- $\gamma$ -positive cells was unaffected by CD4<sup>LVFOXP3</sup> cell administration. Similarly, the proliferation against candida was detected after *in vitro* re-challenge and was not affected by CD4<sup>LVFOXP3</sup> cell administration (Figure 7c). Both IFN- $\gamma$  and proliferation were detectable after stimulation with candida but not with tetanus toxoid (negative control). Human CD4<sup>+</sup> T cells still responded to candida 2 weeks after CD4<sup>LVFOXP3</sup> cell injection indicating that CD4<sup>LVFOXP3</sup> cell injection does not interfere with the ability of PBMCs to respond to fungal antigens.

We also tested immunity against viral antigens 2 weeks after CD4<sup>LVFOXP3</sup> cell injection. Donor PBMCs were preselected based on IFN- $\gamma$  production in response to stimulation with a pool of adenovirus peptides (AdV). NSG mice were humanised by co-injection of PBMC and mDC pulsed with AdV peptides. Either autologous CD4<sup>LVFOXP3</sup> or CD4<sup>LVNGFR</sup> cells derived from the same healthy donors were injected 6 days after PBMC injection. IFN- $\gamma$ -positive cells were detected in PBMC restimulated by mDC pulsed with AdV peptides and their frequency was not affected by CD4<sup>LVFOXP3</sup> cell administration (Figure 7d). The

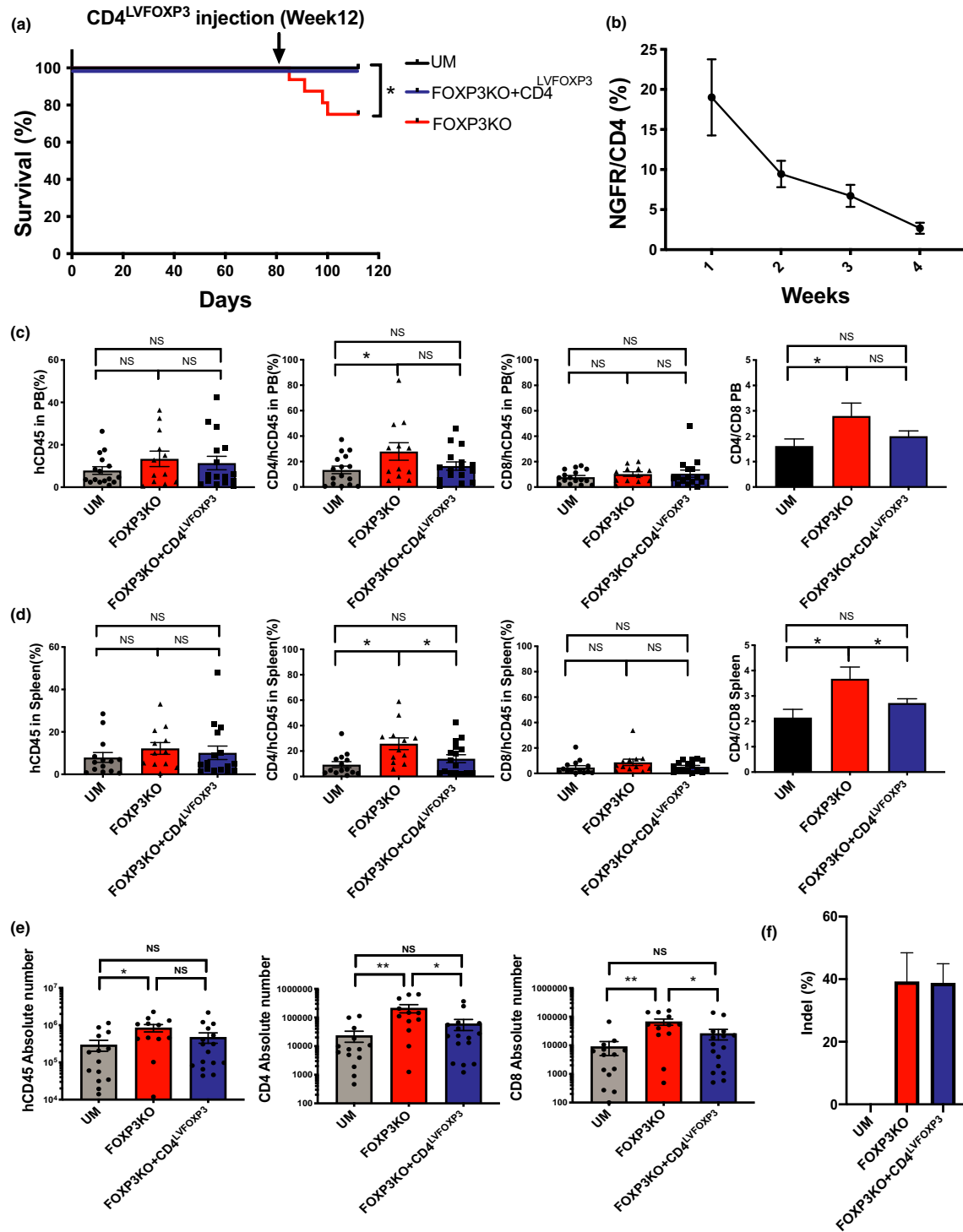


**Figure 6.** CD4<sup>LVFOXP3</sup> cells can ameliorate CD4 dominant lymphoproliferation in *FOXP3* KO hu-mice. **(a)** Survival of *FOXP3* KO hu-mouse model comparing mice transplanted with unmodified HSPC (UM), *FOXP3* KO HSPC alone or plus CD4<sup>LVFOXP3</sup> cells ( $n = 16$ ). **(b)** Percentage of NGFR<sup>+</sup> cells in human CD4<sup>+</sup> cells in PB ( $n = 16$ , mean  $\pm$  SEM). **(c)** Percentage of hCD45<sup>+</sup>/CD4<sup>+</sup>/CD8<sup>+</sup> cells in PB ( $n = 12-16$ , mean  $\pm$  SEM). **(d)** Percentage of hCD45<sup>+</sup>/CD4<sup>+</sup>/CD8<sup>+</sup> cells in the spleen ( $n = 12-16$ , mean  $\pm$  SEM). **(e)** Absolute numbers of hCD45<sup>+</sup>/CD4<sup>+</sup>/CD8<sup>+</sup> cells in the spleen ( $n = 12-16$ , mean  $\pm$  SEM). **(f)** Frequency of INDEL was measured by TIDE analysis of PB from *FOXP3* KO hu-mice ( $n = 8-10$ , mean  $\pm$  SEM). Data are representative of two independently repeated experiments. All phenotyping was performed by FACS.  $P$ -values: \* < 0.05, \*\* < 0.01, \*\*\* < 0.001, \*\*\*\* < 0.0001.

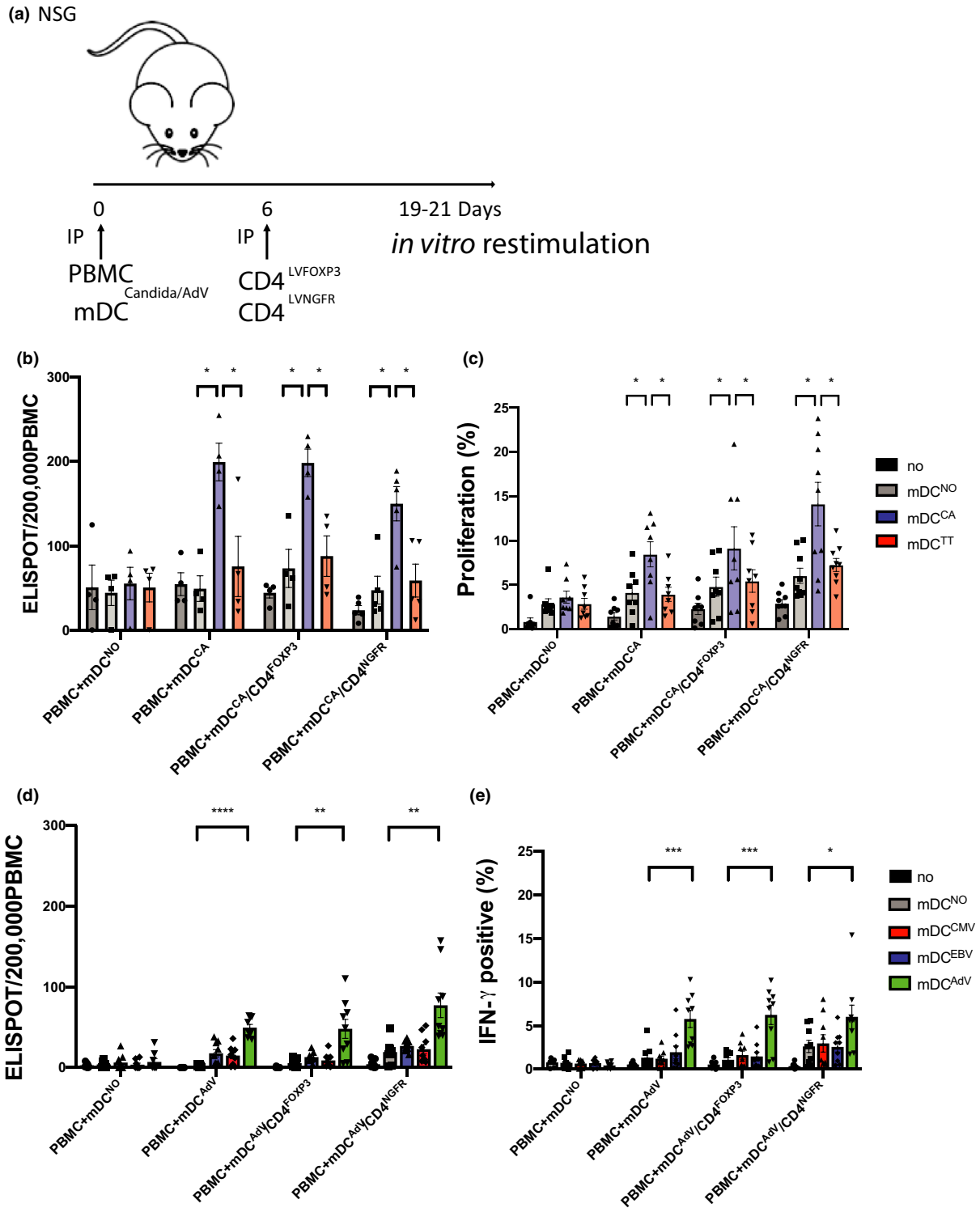


**Figure 7.** Immunity against various pathogens is preserved after CD4<sup>LVFOXP3</sup> cells administration. (a) Design of the experiment to test immune response against fungal (*Candida albicans*) or viral antigens (Adenovirus). Results after *in vitro* restimulation in the presence of mDC pulsed with different antigens are shown. (b) Frequency of IFN- $\gamma$ -positive cells counted by ELISpot ( $n = 4$  or  $5$ , mean  $\pm$  SEM). (c) Proliferation of CD4<sup>+</sup> T cells ( $n = 8$  or  $9$ , mean  $\pm$  SEM). (d) Frequency of IFN- $\gamma$ -positive cells counted by ELISpot ( $n = 8$  or  $9$ , mean  $\pm$  SEM). (e) Frequency of IFN- $\gamma$ -positive cells ( $n = 8$  or  $9$ , mean  $\pm$  SEM). Data are representative of two independently repeated experiments. no = T cells only, NO = no antigen, CA = *Candida albicans*, TT = tetanus toxoid (negative control), Adv = Adenovirus, EBV = Epstein-Barr virus (negative control), CMV = Cytomegalovirus (negative control).  $P$ -values: \*  $< 0.05$ , \*\*  $< 0.01$ , \*\*\*  $< 0.001$ , \*\*\*\*  $< 0.0001$ .

IFN- $\gamma$  expression of human CD4<sup>+</sup> and CD8<sup>+</sup> T cells was measured 6 h after *in vitro* restimulation (Figure 7e). Human CD4<sup>+</sup> and CD8<sup>+</sup> T cells were still able to respond to viral antigens 2 weeks after CD4<sup>LVFOXP3</sup> cell injection.

These data indicate that in this hu-mouse model primed antifungal and antiviral responses are maintained in the presence of CD4<sup>LVFOXP3</sup> cells.

### Immune surveillance against tumor is preserved after CD4<sup>LVFOXP3</sup> cell administration

To test whether CD4<sup>LVFOXP3</sup> cells hinder immune reactions against tumor antigens, a skin sarcoma model was established by subcutaneous injection of myeloid cell line (ALL-CM) in NSG mice.<sup>22</sup> To monitor tumor growth, the luciferase reporter gene (LUC) was transduced by PiggyBac transposase into ALL-CM (ALL-CM<sup>LUC</sup>). Three days after subcutaneous injection of ALL-CM<sup>LUC</sup>, PBMCs were subcutaneously co-injected with either autologous CD4<sup>LVFOXP3</sup> or CD4<sup>LVNGFR</sup> cells. Tumor growth was monitored by direct measurement (every 3 days until day 21) and *in vivo* imaging system (IVIS); every 7 days until day 19 (Figure 8a).

Based on the direct measurement of tumor size, neither CD4<sup>LVFOXP3</sup> nor CD4<sup>LVNGFR</sup> cells interfered with tumor clearance mediated by PBMCs (Figure 8b). Tumor growth measured by IVIS was inhibited by PBMC injection. Importantly, co-injection of CD4<sup>LVFOXP3</sup> or CD4<sup>LVNGFR</sup> cells was permissive to PBMC-induced ALL-CM<sup>LUC</sup> tumor elimination, as confirmed by the reduction in luciferase expression (Figure 8c). Both sarcoma weight (mg) and volume (mm<sup>3</sup>) were also significantly reduced by PBMC injection, and co-injection of CD4<sup>LVFOXP3</sup> or CD4<sup>LVNGFR</sup> cells did not interfere with this antitumor effect (Figure 8d and e). These results indicate that PBMC-induced immune reactions against tumor antigens are not hampered by CD4<sup>LVFOXP3</sup> cell injection.

## DISCUSSION

Treg cell therapy has gained considerable attention and demonstrated safety in recently completed phase I clinical trials.<sup>7</sup> While its clinical use currently extends from indications in GvHD to autoimmune diseases such as T1D, rheumatoid arthritis, autoimmune skin diseases and solid organ transplantations (ClinicalTrials.gov), ongoing experimental efforts are devoted to

improving Treg product generation and manufacturing, in particular using gene modifications to enhance feasibility, survival, stability and efficacy. We previously described a novel Treg-like cell product, CD4<sup>LVFOXP3</sup> cells, generated by *FOXP3* gene transfer, that showed great promise for clinical application.<sup>10,11</sup> CD4<sup>LVFOXP3</sup> cells are CD4<sup>+</sup> T cells that acquire suppressive features and functions that resemble those of naturally occurring Tregs, either fresh or *in vitro* expanded.<sup>10,23</sup> We hypothesise that the clinical use of CD4<sup>LVFOXP3</sup> cells will be beneficial to control immune dysregulation in patients with IPEX syndrome, a prototype monogenic multiorgan autoimmune disease, and in other immune-mediated pathologies that could benefit from administration of autologous or allogeneic functionally stable and traceable Treg-like cells. Here, we present an extensive analysis of the molecular and functional features of CD4<sup>LVFOXP3</sup> cells, including their *in vivo* function in hu-mouse models. Importantly, we have established a humanised IPEX-like mouse model to demonstrate that CD4<sup>LVFOXP3</sup> cells can control the proliferation of FOXP3 defective memory Tregs *in vivo*. Additionally, we show that immune suppression by CD4<sup>LVFOXP3</sup> cells is conferred without compromising immune responses to pathogens or tumor antigens in hu-mouse models, thus addressing a major safety concern that Treg cell therapy may induce generalised immunosuppression, and supporting progression to clinical application for phase I safety studies in humans. Our comparative transcriptome analysis shows that CD4<sup>LVFOXP3</sup> cells are transcriptionally distinct from primary Tregs; however, among the genes that are upregulated in CD4<sup>LVFOXP3</sup> cells, we found core Treg transcripts, including those encoding known surface Treg markers. Interestingly, CD4<sup>LVFOXP3</sup> cells acquire Treg-like functions despite remaining methylated at the genomic Treg-specific demethylated region (TSDR), an evolutionarily conserved non-coding element within the *FOXP3* gene locus that must be demethylated for genomic *FOXP3* gene expression.<sup>24</sup> These data confirm that LV-derived *FOXP3* addition to Tregs induces Treg-like regulatory functions, without initiating complete lineage reprogramming.<sup>23</sup>

Our analysis of the CD4<sup>LVFOXP3</sup> transcriptome and protein expression not only includes the expression of known Treg-associated proteins, but also reveals genes not previously assigned key

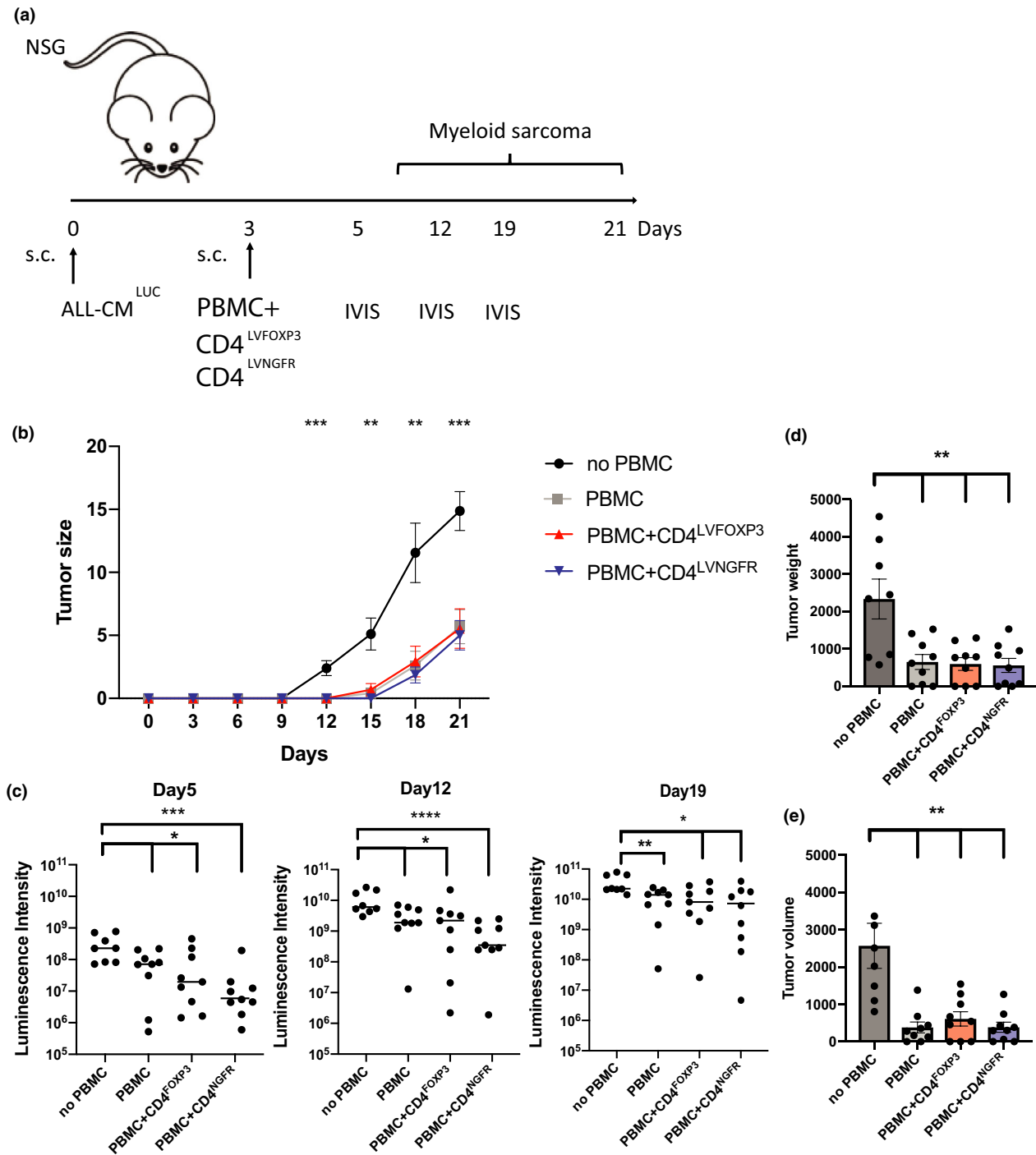


**Figure 8.** Immune surveillance against tumor antigen is preserved after CD4<sup>LVFOXP3</sup> cells administration. **(a)** Design of the experiment to test immune surveillance against tumor antigens. **(b)** Tumor size measured every 3 days by direct measurement ( $n = 8$  or  $9$ , mean  $\pm$  SEM). **(c)** Luminescence intensity (ROI) of skin sarcoma measured weekly by *in vivo* imaging system (IVIS) ( $n = 8$  or  $9$ , median). **(d)** Tumor weight (mg) measured after isolation of skin sarcoma ( $n = 8$  or  $9$ , mean  $\pm$  SEM). **(e)** Tumor volume (mm<sup>3</sup>) calculated after isolation of skin sarcoma ( $n = 8$  or  $9$ , mean  $\pm$  SEM). Data are representative of two independently repeated experiments. *P*-values: \* < 0.05, \*\* < 0.01, \*\*\* < 0.001, \*\*\*\* < 0.0001.

roles in Treg function. These putative Treg genes open the possibility of future studies aimed at elucidating their function in Treg biology. Specific examples include *MEOX1*,<sup>14</sup> *TJP3*,<sup>15</sup> *TBC1D4*<sup>16</sup> and *F5*,<sup>13</sup> all of which have ill-defined roles in Tregs in mice or humans. Their observed upregulation in T cells upon ectopic expression of FOXP3 may suggest that their expression is FOXP3-dependent. However, whether this is a direct or indirect effect has not been resolved. Furthermore, the role of these genes in functional and/or metabolic activities of human Tregs<sup>25</sup> requires further investigation. Future analyses will include a comparison of the transcriptomic profiles from CD4<sup>LVFOXP3</sup> cells to that of activated, expanded Tregs, which are currently used as Treg cell product in the clinic. This comparison could shed light on functionally important genes and on genes that are downregulated in response to FOXP3 expression, which might be more evident in activated compared to fresh Tregs.<sup>13</sup> The analysis of the TCR $\beta$  sequences of CD4<sup>LVFOXP3</sup> cells prior to and after transduction demonstrates that the TCR is unchanged during the *in vitro* CD4<sup>LVFOXP3</sup> cell generation. Thus, in contrast to freshly isolated Tregs, which have a distinct and non-overlapping TCR repertoire compared to Teffs,<sup>26,27</sup> our results demonstrate that CD4<sup>LVFOXP3</sup> cells maintain a TCR repertoire that is similar to that of the parental Teffs. This finding suggests that autoreactive pathogenic Teffs, likely abundant in patients with autoimmune manifestations,<sup>28,29</sup> could also be converted to Treg-like cells using the LV-FOXP3 gene transfer technology.

Despite the broad interest in Treg cell therapy, *in vivo* experimental models to address efficacy and safety questions have been limited.<sup>30</sup> The *in vivo* studies we show here in humanised mice provide experimental evidence and translatable information for Treg clinical use, especially in autoimmune diseases. For example, the efficacy and survival of autologous vs allogeneic Tregs have been difficult to assess, especially in non-immune compromised hosts. *In vivo* survival up to 1 year has been shown when very high doses of autologous Tregs have been administered in T1D.<sup>6</sup> Our data are in line with the view that autologous Tregs have a significant advantage, including longer survival. Similarly, gene integration studies by deep sequencing in blood of SCID patients treated many years before with autologous gene-modified T cells showed their

persistence in peripheral blood for as long as 12 years.<sup>31</sup> By contrast, our data also suggest that alloreactivity by the responder cells could limit allogeneic CD4<sup>LVFOXP3</sup> cells survival *in vivo*. Taking all of these findings together, we are confident that autologous CD4<sup>LVFOXP3</sup> cells will have a sustained *in vivo* survival.

The xeno-GvHD protective effects of Tregs are explained by their persistence in the periphery and/or tissues, and by changes in the immune microenvironment.<sup>20</sup> Our data support the likelihood of a similar effect for CD4<sup>LVFOXP3</sup> cells on the surrounding immune cells, since the protection from xeno-GvHD was associated with lower expression of T-cell activation markers. This protection was observed upon re-challenge with the same Teffs, even when CD4<sup>LVFOXP3</sup> cells were no longer detected in the peripheral blood of the injected mice, and is consistent with the observation that post-HSCT patients receiving *in vitro* expanded Tregs have lower GvHD, despite the fact that the Tregs were detectable for only a few weeks after their administration.<sup>32–34</sup>

Most importantly, our FOXP3-deficient hu-mouse is a valuable model, though with some aspects to be improved, in which the regulatory effect of CD4<sup>LVFOXP3</sup> cells on an intrinsically dysregulated immune system can be demonstrated, mimicking what happens in IPEX patients when Teffs-Tregs balance is lost. Previously, hu-mice (NOD.*Prkdc*<sup>scid</sup>*Il2r $\gamma$* <sup>-/-</sup>*H2-Ab1*<sup>-/-</sup>Tg) expressing human HLA class II reconstituted with HSPCs from one IPEX patient were shown to develop multiple autoimmune pathologies which resembled those of IPEX syndrome.<sup>35</sup> In the present study, to avoid the need of patients' T cells and HSPCs matching the HLA type of the mouse model, we established a more versatile FOXP3-deficient hu-mouse model to validate the efficacy and robustness of autologous CD4<sup>LVFOXP3</sup> cells made from multiple donors, although the lack of human HLA class II in the recipient mice, limited the development of IPEX-like tissue aggression. In the IPEX-like *FOXP3* KO hu-mouse model, multilineage engraftment occurs normally but the human immune system differentiates aberrantly, leading to reduced Tregs and increased T-cell proliferation, especially of the CD4<sup>+</sup> memory T cells. The *FOXP3* KO hu-mice display mild CD4<sup>+</sup> T-cell infiltration in the gut, which is the major target organ in IPEX syndrome patients and other immunodysregulatory diseases.<sup>36</sup> Our *FOXP3* KO hu-mice showed significantly higher mortality

compared to the control; however, this was less than that reported for hu-mice in which the recipient mice are transgenic for the human HLA class II molecules and are transplanted with HLA-matched IPEX patient HSPCs.<sup>35</sup> Therefore, although informative, the IPEX-like model we have generated is not complete in recapitulating the full severe IPEX clinical phenotype and in abrogating completely FOXP3 expression. To obtain a more robust self-specific tissue infiltration and organ aggression, a mouse strain such as NSG mice, which express human MHC class II molecules (such as HLA-DR1 or HLA-DR4) would need to be used. To test the efficacy of the CD4<sup>LVFOXP3</sup> cells in such a model, the HLA types of HSC donors and mice have to be matched. An attempt that was not feasible at this time. To repopulate the mouse with human cells completely lacking FOXP3 expression, cells would need sequential editing, first CRISPR/Cas9 KO of FOXP3, followed by the knock-in of the AAV6 construct-expressing NGFR, allowing purification and *in vivo* injection of pure FOXP3 KO cells.<sup>12</sup> This set of experiments requires large numbers of HSPCs (autologous to the T cells from which CD4<sup>LVFOXP3</sup> cells are generated) which are difficult to obtain in a research setting but would be feasible in a preclinical development context. Overall, the IPEX-like model presented has some of the key characteristics of the aberrant T-cell system in IPEX (CD4<sup>+</sup> lymphoproliferation, memory T-cell expansion and Treg reduction), and our data show that the administration of CD4<sup>LVFOXP3</sup> cells can prevent these pathologies. Injection of CD4<sup>LVFOXP3</sup> cells rescued the phenotype of FOXP3 KO hu-mice by preventing the increase in CD4<sup>+</sup> T cells and normalising the CD4/CD8 ratio and the naïve/memory proportion. At the same time, CD4<sup>LVFOXP3</sup> cells did not impact the total human cell engraftment or multilineage engraftment, further supporting the regulatory function of CD4<sup>LVFOXP3</sup> cells while suggesting that they could safely promote immune homeostasis, even in a FOXP3-deficient environment. These are informative data, especially considering that, although autoimmunity in IPEX has a very wide phenotypic variability, the T-cell compartment is consistently impacted.

Although Tregs exert a non-redundant role in protection from immune pathology, it has been speculated that their function can be detrimental for antiviral/fungal immune responses and antitumor immunity. Indeed, several examples

have been reported in which Tregs prevent clearance of infections<sup>37,38</sup> or favor tumor escape mechanisms.<sup>39,40</sup> Therefore, although freshly isolated or expanded polyclonal Tregs administered in patients after HSCT or in T1D did not lead to a subsequent increased incidence of infections,<sup>5,6</sup> it was important to address the possibility that CD4<sup>LVFOXP3</sup> cell infusion may dampen pathogen immune response and immune surveillance. The experiments we performed showed that the injection of CD4<sup>LVFOXP3</sup> cells shortly after antigen (candida and adenovirus) priming did not impair expansion and persistence of Ag-specific T cells, and the Ag-specific T cells were responsive after re-challenge with the same Ag *in vitro*. The observed persistence of Ag-specific T cell suggests they could expand *in vivo* and that there is no impact on immune responses by the injected CD4<sup>LVFOXP3</sup>. However, this result does not address the effect of CD4<sup>LVFOXP3</sup> cells on the actual initiation of the immune response and priming, because the CD4<sup>LVFOXP3</sup> cell infusion was performed shortly after priming (day 6 after human responder T cells/pulsed mDC transfer). The current infection model of expansion of primed Ag-specific T cells requires that the mouse is not irradiated (to limit the irradiation-mediated inflammatory xeno-GvHD reaction which would mask the actual Ag-specific response). In that setting, co-injection of the CD4<sup>LVFOXP3</sup> cells together with the T cells/pulsed mDC prevented engraftment (not shown). However, from our previous published experiments, in which we tested the effect of CD4<sup>LVFOXP3</sup> cells injected at day 6 (late transfer) in the control of xeno-GvHD (after irradiation), we observed protective effects without engraftment prevention.<sup>11</sup> Based on these parallel data, we established that day 6 CD4<sup>LVFOXP3</sup> cell transfer was still within the time frame to assess the effect of CD4<sup>LVFOXP3</sup> cells towards host immunity against pathogens, and, at the same time, allows the primed responder cells to engraft. Therefore, overall our data provide evidence that while suppressing xeno-GvHD, the CD4<sup>LVFOXP3</sup> cells do not impair response to pathogens, showing a more selective effect as compared to pharmacological immunosuppression.

Similarly, the injection of CD4<sup>LVFOXP3</sup> cells did not impair tumor clearance by co-injected PBMCs. These *in vivo* data confirm that CD4<sup>LVFOXP3</sup> cells do not dampen the beneficial immune response. It might be difficult to draw a general conclusion

from a single cancer xenograft model. However, the cancer model that we have used to assess the impact of Treg-like cells is commonly accepted for evaluating tumor clearance<sup>22</sup>; thus, we have adopted it to exclude the inhibition of tumor clearance after Treg-like cell injection.

In conclusion, CD4<sup>LVFOXP3</sup> cells can be reproducibly generated from autologous CD4<sup>+</sup>T cells, which pose no limitations in isolation and expansion *in vitro*. High levels of CD4<sup>LVFOXP3</sup> cell purity can be guaranteed by isolation of transduced cells via the co-expressed *NGFR* surface marker, which can be also used for *in vivo* tracking. The molecular and functional results reported here indicate that CD4<sup>LVFOXP3</sup> cells have essential attributes of Treg cells and that their function is stable even in an immune-dysregulated environment. Moreover, we provide compelling evidence that, in the hu-mouse model we used, the presence of CD4<sup>LVFOXP3</sup> cells does not abrogate ongoing immune responses to pathogen or tumor antigen clearance. Therefore, CD4<sup>LVFOXP3</sup> cells hold great clinical promise as a next-generation engineered Treg therapy in immune-dysregulated diseases, including but not limited to IPEX syndrome, to replace dysfunctional or insufficient Tregs.

Collectively, these data support near-term initiation of a phase I first-in-human trial in IPEX syndrome to assess safety.

## METHODS

### Cell purification and CD4<sup>+</sup> T-cell culture

Buffy coats from healthy donors were provided from Stanford Blood Center. PBMCs were separated from the buffy coat by density gradient centrifugation using Ficoll-Paque (GE Healthcare Science, Chicago, IL, USA). CD4<sup>+</sup> T cells were enriched from PBMCs by negative selection (STEMCELL Technologies, Vancouver, BC, Canada). CD4<sup>+</sup> T cells were cultured by X-VIVO 15 Medium supplemented with gentamicin (Lonza, Basel, Switzerland) and 5% human serum from pooled male AB plasma (Sigma-Aldrich, St Louis, MO, USA).

### Lentiviral production

The original bidirectional lentiviral vector expressing *FOXP3* (pCCL-FOXP3, 10.7kb) was modified to improve safety and production efficiency. These modifications included removal of the N-terminal hemagglutinin (HA) tag to avoid potential immunogenicity, and removal of the LacZ and F1 origin cassettes in the vector backbone to reduce the plasmid size (LV-FOXP3; 10.0 Kb; Supplementary figure 1a).

As a control, the *FOXP3* gene was removed to generate a vector expressing only the marker gene (LV-NGFR).

Lentivirus was produced as previously described.<sup>10,11</sup> Briefly, vector plasmid (pCCL-FOXP3/LV-FOXP3 or control LV-NGFR) and helper plasmids (gag/pol, REV, VSVG and pAdVantage) were transiently co-transfected to HEK293T/17 cells (ATCC, Manassas, VA, USA) by Mirus LT1 Reagent (Mirus Bio LLC, Madison, WI, USA). The supernatant was collected 30 h after transfection and concentrated by ultracentrifugation. Titre of lentivirus was determined by limiting dilution. Overall high-titre LVs were generated using the modified LV constructs (LV-FOXP3 1.34\*10<sup>9</sup> TU mL<sup>-1</sup>, LV-NGFR 1.61\*10<sup>9</sup> TU mL<sup>-1</sup>, mean, *n* = 4).

### CD4<sup>+</sup> T-cell transduction

For transduction, freshly isolated CD4<sup>+</sup> T cells were activated overnight by allogeneic CD3 depleted PBMC (allogeneic APC) with 100 U mL<sup>-1</sup> IL-2 and 10 ng mL<sup>-1</sup> IL-7. On day 1, lentivirus was added to the activated T cells at the MOI of 20. Cells were split every 2–3 days. Similar transduction efficacy can be observed in CD4<sup>+</sup> T cells between LV-FOXP3 and LV-NGFR (CD4<sup>LVFOXP3</sup> cells 75.2%, CD4<sup>LVNGFR</sup> cells 82.2%, mean, *n* = 8). On days 9–10, transduced CD4<sup>+</sup> T cells were enriched by MACSelect LNGFR System (Miltenyi Biotec, Bergisch Gladbach, Germany). While transduction efficiency is comparable for both LVs, CD4<sup>LVFOXP3</sup> cells expanded slower than CD4<sup>LVNGFR</sup> cells after the first round of expansion (CD4<sup>LVFOXP3</sup> cells 3.76-fold increase, CD4<sup>LVNGFR</sup> cells 8.70-fold increase, mean, *n* = 8; Supplementary figure 1b).

On day 14, transduced CD4<sup>+</sup> T cells are restimulated by feeder cell mixture (10<sup>6</sup> PBMCs mL<sup>-1</sup> and 10<sup>5</sup> JY cells mL<sup>-1</sup>). Phenotype and function of transduced CD4<sup>+</sup> T cells were analysed 9–11 days after restimulation. Vector copy number was measured by real-time PCR with no significant difference in VCN between the transduced cells (CD4<sup>LVFOXP3</sup> cells 1.80 VCN cell<sup>-1</sup>, CD4<sup>LVNGFR</sup> cells 2.86 VCN cell<sup>-1</sup>, mean, *n* = 8; Supplementary figure 1c).

### RNA-seq

RNA-seq was performed on isolated RNA from CD4<sup>LVFOXP3</sup> and CD4<sup>LVNGFR</sup> cells. RNA was also isolated from freshly isolated Tregs (CD25<sup>+</sup>CD127<sup>-</sup>) and non-Tregs (CD4<sup>+</sup>CD25<sup>-</sup>) from the same donor generated in parallel. Briefly, purified RNA was assessed for quantity and quality using an Agilent 2100 Bioanalyzer and Qubit Instrument. RNA-seq libraries were generated using Illumina TruSeq Stranded Total RNA Kits (Illumina, San Diego, CA, USA). The resultant cDNA libraries were quantified via Qubit and assessed for quality via Bioanalyzer. Libraries were molecularly barcoded, pooled at equimolar concentrations and sequenced at 2 × 100 cycles on an Illumina HiSeq 2500.

### Vector copy number

Genomic DNA was extracted from 1 million of CD4<sup>+</sup> T cells by DNeasy Blood and Tissue Kit (Qiagen, Hilden, Germany). Vector copy number was measured by Lenti-X Provirus Quantification Kit (Takara Bio, Mountain View, CA, USA) according to the manufacturer's protocol.

## TCR sequencing

Genomic DNA was extracted from 0.1 million of CD4<sup>+</sup> T cells by DNeasy Blood and Tissue Kit (Qiagen). TCR sequencing was done by immunoSEQ TCR beta assay and analysed by immunoSEQ analyzer (Adaptive Biotechnologies, Seattle, WA, USA). TCR Clonality index was calculated and shown by the Clonality index, where  $R$  = the total number of rearrangements;  $x$  = each rearrangement; and  $P(x)$  = productive frequency of rearrangement ( $x$ ).

$$\text{Clonality Index} \equiv 1 - \frac{-\sum_{x=1}^R P(x) \log_2 [P(x)]}{\log_2 R}$$

## Flow cytometry (FACS)

CD4<sup>+</sup> T cells were resuspended in FACS buffer (PBS supplemented with 0.5% BSA and 2 mM EDTA) and stained using an antibody cocktail for 30 min. After surface staining, intracellular staining (FOXP3 and CTLA4) was performed with the Foxp3/Transcription Factor Staining Buffer Set (eBioscience, San Diego, CA, USA). Data were acquired by FACSARIA II (BD Biosciences, San Jose, CA, USA) and analysed by FlowJo 10.4 software (FlowJo LLC, San Jose, CA, USA). Antibody list is provided in Supplementary table 5.

## qPCR

Total RNA was extracted from one million of CD4<sup>+</sup> T cells by RNeasy Plus Mini Kit (Qiagen). 100 ng of RNA was used to synthesise cDNA by SuperScript IV VILO (Thermo Fisher Scientific, Waltham, MA, USA). qPCR was done by TaqMan Gene Expression Assay and TaqMan Universal Master Mix II (Thermo Fisher). Gene expression was calculated by  $\Delta\text{CT}$ , where  $\Delta\text{CT} = \text{CT}_{\text{target}} - \text{CT}_{\text{housekeeping}}$ . The internal control housekeeping gene is *HPRT*. The qPCR primer (TaqMan Gene Expression Assay) list is shown in Supplementary table 6.

## Cytokine production

CD4<sup>+</sup> T cells were cultured at a density of one million of cells mL<sup>-1</sup> in a round-bottom 96-well plate and activated using the Dynabeads Human T-cell Activator CD3/CD28 (Gibco, Gaithersburg, MD) at a 1:25 bead:cell ratio. Culture supernatant was collected at 24 h (IL-2) and 72 h (IL-4, IFN- $\gamma$ , IL-17A, IL-22) after stimulation. Cytokine concentrations including IL-2, IL-4 and IFN- $\gamma$  were measured by Human OptEIA ELISA Kit (BD Bioscience). Cytokine concentrations including IL-17A and IL-22 concentrations were measured by Human DuoSet ELISA Kit (R&D Systems, Minneapolis, MN, USA).

## Proliferation and suppression assay

The proliferation assay was performed as previously described<sup>11</sup> CD4<sup>+</sup> T cells labelled by CellTrace CFSE (Life Technologies, Carlsbad, CA, USA) were activated by

Dynabeads Human T-cell Activator CD3/CD28 at 1:25 bead:cell ratio. After 96 hours of stimulation, the proliferation of CD4<sup>+</sup> T cells was counted by FACS.

The suppression assay was performed as previously described.<sup>11</sup> Briefly, responder CD4<sup>+</sup> T cells (50 000 cells) labelled by CFSE and suppressor CD4<sup>+</sup> T cells (12 500–50 000 cells) labelled by CellTrace Violet (Life Technologies) were co-cultured at different concentrations (1:0.25–1:1) after activation by Dynabeads Human T-cell Activator CD3/CD28 at 1:25 bead:cell ratio. After 96 hours of stimulation, the proliferation of responder CD4<sup>+</sup> T cells was counted by FACS.

## The xeno-GvHD mouse model

A xeno-GvHD mouse model was created by intraperitoneal injection of human two millions of CD4<sup>+</sup> T cells in 6- to 8-week-old female NSG mice after sublethal irradiation (2Gy). Either two millions of autologous/allogeneic CD4<sup>LVFOXP3</sup> or autologous CD4<sup>LVNGFR</sup> cells were co-injected (allogeneic CD4<sup>LVFOXP3</sup> cells  $n=7$ , autologous CD4<sup>LVFOXP3</sup> cells  $n=8$ , autologous CD4<sup>LVNGFR</sup> cells  $n=7$ , Teff  $n=8$ ). xeno-GvHD mice were re-challenged with the same responder Teff ( $2 \times 10^6$  cells) 2 weeks after the initial co-injection of Teff and autologous CD4<sup>LVFOXP3</sup> (re-challenge condition). Control mice in which we injected Teff 2 weeks after sublethal irradiation were tested in parallel (Teff-late condition; autologous CD4<sup>LVFOXP3</sup> cells  $n=8$ , autologous CD4<sup>LVFOXP3</sup> cells +re-challenge  $n=9$ , autologous CD4<sup>LVNGFR</sup> cells  $n=8$ , Teff  $n=8$ , Teff-late  $n=8$ ). The experimental protocol was approved by Stanford University's Administrative Panel on Lab Animal Care. Body weight and survival were monitored every 2–3 days. PBMC was obtained weekly by retro-orbital bleeding. Six weeks after injection, mice were sacrificed and spleen was analysed by FACS.

## TheFOXP3 knockout hu-mouse model

The *FOXP3* gene was disrupted by CRISPR/Cas9-mediated non-homologous end joining. Freshly isolated cord blood-derived CD34<sup>+</sup> hematopoietic stem cell was expanded for 2 days with cytokine cocktails (100 ng mL<sup>-1</sup> Flt3L, 100 ng mL<sup>-1</sup> SCF, 100 ng mL<sup>-1</sup> TPO, 100 ng mL<sup>-1</sup> IL-6, 35 nM UM-171 and 0.75  $\mu\text{M}$  SR-1). The RNP complex was created by incubation of the sgRNA targeting FOXP3 (TriLink BioTechnologies, San Diego, CA, USA) with Cas9 protein (Integrated DNA Technologies, Coralville, IA, USA) at room temperature for 15 min. The RNP complex was electroporated into HSPC by Nucleofector (Lonza); transfected cells were expanded for 2 days. As an unmodified control, CD34<sup>+</sup> HSPCs were cultured in parallel without transfection of RNP complex. 150 000 of *FOXP3* KO HSPCs were intrahepatically transplanted to the neonatal NSG mice (days 2–3) after sublethal irradiation (1Gy). Twelve weeks after injection, CD4<sup>LVFOXP3</sup> cells ( $10^6$  cells) generated from the same cord blood donor were injected peritoneally. The experimental protocol was approved by Stanford University's Administrative Panel on Lab Animal Care. PB was obtained biweekly by retro-orbital bleeding. Sixteen weeks after injection, mice were sacrificed and spleen was analysed by FACS.

## Histology

Mouse tissues were immediately fixed by 10% formalin solution (Sigma-Aldrich) after sample collection. On the next day, the fixed sample was transferred to 70% ethanol and kept until sectioning. The preparation of the slide and immunostaining was done by HistoWiz (HistoWiz Inc, Brooklyn, NY, USA). Anti-human CD4 antibody was used for immunostaining.

## The PBMC hu-mouse model of antigen-specific immune response

PBMCs isolated from buffy coat were stained with CFSE and stimulated with  $1 \mu\text{g mL}^{-1}$  of *C. albicans* or tetanus toxoid. The proliferation of CD4<sup>+</sup> T cells was measured between 4 and 6 days after antigen pulse; PBMC donors who showed > 5% proliferation against *C. albicans* and tetanus toxoid were considered to be positive responders. PBMCs ( $7.5 \times 10^6$  cells) from positive responders against either *C. albicans* or tetanus toxoid were injected intraperitoneally in 6- to 8-week-old NSG mice together with mDC pulsed with *C. albicans* ( $7.5 \times 10^5$  cells). Six days after PBMC injection, CD4<sup>LVFOX P3</sup> cells ( $10^6$  cells) were injected intraperitoneally (PBMC<sup>+</sup>mDC<sup>NO</sup>  $n = 8$ , PBMC<sup>+</sup>mDC<sup>CA</sup>  $n = 8$ , PBMC<sup>+</sup>mDC<sup>CA</sup>+CD4<sup>LVFOX P3</sup> cells  $n = 8$ , PBMC<sup>+</sup>mDC<sup>CA</sup>+CD4<sup>LVNGFR</sup> cells  $n = 9$ ). The experimental protocol was approved by Stanford University's Administrative Panel on Lab Animal Care. Mice were sacrificed 19–21 days after PBMC injection, and splenocytes were collected. Murine cells were depleted by negative isolation, and enriched human PBMCs were restimulated by mDC pulsed with *C. albicans* or tetanus toxoid. IFN- $\gamma$ -positive cells were counted by ELISpot assay. The proliferation of CD4<sup>+</sup> T cells in human PBMC was measured 4 days after restimulation.

PBMCs isolated from buffy coat were stimulated with  $1 \mu\text{g mL}^{-1}$  of viral peptide (adenovirus, CMV and EBV), and IFN- $\gamma$ -positive cells were counted by FACS. PBMCs ( $7.5 \times 10^6$  cells) from positive responders against adenovirus were injected intraperitoneally in 6- to 8-week-old NSG mice together with mDC pulsed with adenovirus peptide ( $7.5 \times 10^5$  cells). Six days after PBMC injection, CD4<sup>LVFOX P3</sup> cells ( $10^6$  cells) were injected intraperitoneally (PBMC<sup>+</sup>mDC<sup>NO</sup> cells  $n = 8$ , PBMC<sup>+</sup>mDC<sup>Adv</sup> cells  $n = 9$ , PBMC<sup>+</sup>mDC<sup>Adv</sup>+CD4<sup>LVFOX P3</sup> cells  $n = 9$ , PBMC<sup>+</sup>mDC<sup>Adv</sup>+CD4<sup>LVNGFR</sup> cells  $n = 9$ ). The experimental protocol was approved by Stanford University's Administrative Panel on Lab Animal Care. Mice were sacrificed 19–21 days after PBMC injection, and splenocyte was collected. Murine cells were depleted by negative isolation, and enriched human PBMCs were restimulated by mDC pulsed with viral peptide (adenovirus, CMV and EBV). IFN- $\gamma$ -positive cells were counted by FACS and ELISpot assay.

## ELISpot

The IFN- $\gamma$  ELISpot (R&D Systems) was carried out according to the manufacturer's protocol. Briefly,  $2 \times 10^5$  PBMC stimulated with  $2 \times 10^4$  mDC loaded with specific antigen overnight. The next day, IFN- $\gamma$  was captured and detected

and the number of the positive colony in each experimental condition was counted automatically by ImmunoSpot analyzer (Cellular Technology Limited, Cleveland, OH).

## PiggyBac transfection

ALL-CM was kindly provided by Dr Silvia Gregori [San Raffaele Telethon Institute for Gene Therapy (SR-TIGET), IRCCS San Raffaele Scientific Institute]. To generate ALL-CM expressing luciferase, the ALL-CM cells were nucleofected by Amaxa 4D-Nucleofector System with X Unit (Lonza) using EP-100 program. In brief,  $5 \times 10^5$  ALL-CM cells were resuspended in a solution containing 100  $\mu\text{L}$  of SF medium and 1  $\mu\text{g}$  of PiggyBac transposon expression vector (luciferase–puromycin) and 2  $\mu\text{g}$  of PiggyBac transposase expression vector kindly provided by Dr Yasuhiro Takashima (Cambridge University). After 3 weeks of puromycin selection, cells were frozen until *in vivo* use.

## The PBMC hu-mouse model of skin sarcoma

ALL-CM<sup>LUC</sup> ( $2 \times 10^6$  cells) was subcutaneously injected in 6- to 8-week-old NSG mice. The experimental protocol was approved by Stanford University's Administrative Panel on Lab Animal Care. On day 3, PBMC ( $2 \times 10^6$  cells) was injected with and without CD4<sup>LVNGFR</sup>/CD4<sup>LVFOX P3</sup> cells ( $10^6$  cells; no PBMC  $n = 8$ , PBMC  $n = 9$ , PBMC+CD4<sup>LVFOX P3</sup> cells  $n = 9$ , PBMC+CD4<sup>LVNGFR</sup> cells  $n = 9$ ). Body weight and tumor size were measured every 3 days until day 21. On day 21, mice were sacrificed and tumor was isolated to measure the volume and weight.

## Statistical analysis

GraphPad Prism Software ver 7.0 (GraphPad Software, La Jolla, CA, USA) was used for statistical analyses. All statistical analyses were performed with the two-tailed Student *t*-test or Mann–Whitney *U*-test. Mice survival was analysed with the log-rank test. *P*-values < 0.05 were considered to be significant: \* < 0.05, \*\* < 0.01, \*\*\* < 0.001, \*\*\*\* < 0.0001.

## ACKNOWLEDGMENTS

YS received grants from the Japan Society for Promotion of Science (JSPS) (Research Fellowships of Japan Society for the Promotion of Science for Young Scientists (PD) and JSPS Overseas Research Fellowships). YS and RB received a GSK-Stanford Sir James Black Postdoctoral Fellowship Grant from GSK (GlaxoSmithKline LLC; 1250 South Collegeville Rd, Collegeville, PA 19426, USA). RB received the 2019 Scholar Innovator Award from the Harrington Discovery Institute. Patient samples were collected and investigated thanks to the support of an anonymous donor to the Stanford Center for Genetic Immune Diseases (CGID). Part of these results are considered IND-enabling studies supported by a CLIN\_1 Grant to RB from the California Institute for Regenerative Medicine (CIRM). BDP was supported by fellowships from the National Heart, Lung, and Blood Institute (1T32HL098049) and National Institute of Diabetes and

Digestive and Kidney Diseases (1F32DK100072). The Stanford Center for Genomics and Personalized Medicine performed sequencing services under grant 1S10OD020141-01. We thank Eva Rossi Mel (San Raffaele Telethon Institute for Gene Therapy) for setting up initial *in vivo* experimental protocol; Toshinobu Nishimura and Hiromitsu Nakauchi (Stanford University), and Atsushi Miyawaki and Satoshi Iwano (RIKEN) for kindly providing AkaLuc gene and AkaLucmine-HCl (TokeOni); Maria I Garcia-Lloret and Manish J Butte (UCLA) for clinical collaboration; and Robertson Parkman and Rhonda Perriman for contributing to the manuscript with editing and constructive comments.

## AUTHOR CONTRIBUTIONS

**Yohei Sato:** Conceptualization; Data curation; Formal analysis; Funding acquisition; Investigation; Methodology; Validation; Visualization; Writing-original draft; Writing-review & editing. **Laura Passerini:** Investigation; Methodology; Writing-review & editing. **Brian Piening:** Data curation; Formal analysis; Methodology; Resources; Software. **Molly Javier Uyeda:** Data curation; Formal analysis; Software; Writing-review & editing. **Marianne Goodwin:** Methodology; Resources. **Silvia Gregori:** Methodology; Resources. **Michael P Snyder:** Methodology; Resources; Supervision; Writing-review & editing. **Alice Bertaina:** Resources; Writing-review & editing. **Maria-Grazia Roncarolo:** Conceptualization; Supervision; Writing-original draft; Writing-review & editing. **Rosa Bacchetta:** Conceptualization; Funding acquisition; Supervision; Validation; Writing-original draft; Writing-review & editing.

## CONFLICT OF INTEREST

The authors declare no conflict of interest.

## REFERENCES

- Sakaguchi S, Sakaguchi N, Asano M, Itoh M, Toda M. Immunologic self-tolerance maintained by activated T cells expressing IL-2 receptor alpha-chains (CD25). Breakdown of a single mechanism of self-tolerance causes various autoimmune diseases. *J Immunol* 1995; **155**: 1151–1164.
- Sakaguchi S, Miyara M, Costantino CM, Hafler DA. FOXP3<sup>+</sup> regulatory T cells in the human immune system. *Nat Rev Immunol* 2010; **10**: 490–500.
- Hori S, Nomura T, Sakaguchi S. Control of regulatory T cell development by the transcription factor Foxp3. *Science* 2003; **299**: 1057–1061.
- Fontenot JD, Gavin MA, Rudensky AY. Foxp3 programs the development and function of CD4<sup>+</sup>CD25<sup>+</sup> regulatory T cells. *Nat Immunol* 2003; **4**: 330–336.
- Duggleby R, Danby RD, Madrigal JA, Saudemont A. Clinical grade regulatory CD4<sup>+</sup> T cells (Tregs): moving toward cellular-based immunomodulatory therapies. *Front Immunol* 2018; **9**: 252.
- Bluestone JA, Buckner JH, Fitch M et al. Type 1 diabetes immunotherapy using polyclonal regulatory T cells. *Sci Transl Med* 2015; **7**: 315ra189.
- Ferreira LMR, Muller YD, Bluestone JA, Tang Q. Next-generation regulatory T cell therapy. *Nat Rev Drug Discov* 2019; **18**: 749–769.
- Bacchetta R, Barzaghi F, Roncarolo MG. From IPEX syndrome to FOXP3 mutation: a lesson on immune dysregulation. *Ann N Y Acad Sci* 2018; **1417**: 5–22.
- Barzaghi F, Amaya Hernandez LC, Neven B et al. Long-term follow-up of IPEX syndrome patients after different therapeutic strategies: An international multicenter retrospective study. *J Allergy Clin Immunol* 2018; **141**: 1036–1049.e5.
- Allan SE, Alstad AN, Merindol N et al. Generation of potent and stable human CD4<sup>+</sup> T regulatory cells by activation-independent expression of FOXP3. *Mol Ther* 2008; **16**: 194–202.
- Passerini L, Rossi Mel E, Sartirana C et al. CD4<sup>+</sup> T cells from IPEX patients convert into functional and stable regulatory T cells by FOXP3 gene transfer. *Sci Transl Med* 2013; **5**: 215ra174.
- Goodwin M, Lee E, Lakshmanan U et al. CRISPR-based gene editing enables FOXP3 gene repair in IPEX patient cells. *Sci Adv* 2020; **6**: eaaz0571.
- Bhairavabhotla R, Kim YC, Glass DD et al. Transcriptome profiling of human Foxp3<sup>+</sup> regulatory T cells. *Hum Immunol* 2016; **77**: 201–213.
- Zhang Y, Maksimovic J, Naselli G et al. Genome-wide DNA methylation analysis identifies hypomethylated genes regulated by FOXP3 in human regulatory T cells. *Blood* 2013; **122**: 2823–2836.
- Gerriets VA, Kishton RJ, Johnson MO et al. Foxp3 and Toll-like receptor signaling balance Treg cell anabolic metabolism for suppression. *Nat Immunol* 2016; **17**: 1459–1466.
- Arvey A, van der Veeke J, Samstein RM, Feng Y, Stamatoyannopoulos JA, Rudensky AY. Inflammation-induced repression of chromatin bound by the transcription factor Foxp3 in regulatory T cells. *Nat Immunol* 2014; **15**: 580–587.
- MacDonald KN, Piret JM, Levings MK. Methods to manufacture regulatory T cells for cell therapy. *Clin Exp Immunol* 2019; **197**: 52–63.
- Bondanza A, Valtolina V, Magnani Z et al. Suicide gene therapy of graft-versus-host disease induced by central memory human T lymphocytes. *Blood* 2006; **107**: 1828–1836.
- Hannon M, Lechanteur C, Lucas S et al. Infusion of clinical-grade enriched regulatory T cells delays experimental xenogeneic graft-versus-host disease. *Transfusion* 2014; **54**: 353–363.
- Mutis T, van Rijn RS, Simonetti ER et al. Human regulatory T cells control xenogeneic graft-versus-host disease induced by autologous T cells in RAG2<sup>-/-</sup>γC<sup>-/-</sup> immunodeficient mice. *Clin Cancer Res* 2006; **12**: 5520–5525.
- Harui A, Kiertscher SM, Roth MD. Reconstitution of huPBL-NSG mice with donor-matched dendritic cells enables antigen-specific T-cell activation. *J Neuroimmune Pharmacol* 2011; **6**: 148–157.
- Locafaro G, Andolfi G, Russo F et al. IL-10-engineered human CD4<sup>+</sup> Tr1 cells eliminate myeloid leukemia in an HLA class I-dependent mechanism. *Mol Ther* 2017; **25**: 2254–2269.

23. McMurchy AN, Gillies J, Allan SE et al. Point mutants of forkhead box P3 that cause immune dysregulation, polyendocrinopathy, enteropathy, X-linked have diverse abilities to reprogram T cells into regulatory T cells. *J Allergy Clin Immunol* 2010; **126**: 1242–1251.
24. Baron U, Floess S, Wieczorek G et al. DNA demethylation in the human FOXP3 locus discriminates regulatory T cells from activated FOXP3+ conventional T cells. *Eur J Immunol* 2007; **37**: 2378–2389.
25. Charbonnier LM, Cui Y, Stephen-Victor E et al. Functional reprogramming of regulatory T cells in the absence of Foxp3. *Nat Immunol* 2019; **20**: 1208–1219.
26. Golding A, Darko S, Wylie WH, Douek DC, Shevach EM. Deep sequencing of the TCR-β repertoire of human forkhead box protein 3 (FoxP3)<sup>+</sup> and FoxP3<sup>-</sup> T cells suggests that they are completely distinct and non-overlapping. *Clin Exp Immunol* 2017; **188**: 12–21.
27. Ahmadzadeh M et al. Tumor-infiltrating human CD4+ regulatory T cells display a distinct TCR repertoire and exhibit tumor and neoantigen reactivity. *Sci Immunol* 2019; **4**: eaao4310.
28. Babon JA, DeNicola ME, Blodgett DM et al. Analysis of self-antigen specificity of islet-infiltrating T cells from human donors with type 1 diabetes. *Nat Med* 2016; **22**: 1482–1487.
29. Jelcic I, Al Nimer F, Wang J et al. Memory B cells activate brain-homing, autoreactive CD4<sup>+</sup> T cells in multiple sclerosis. *Cell* 2018; **175**: 85–100.e23.
30. Hahn SA, Bellinghausen I, Trinschek B, Becker C. Translating Treg therapy in humanized mice. *Front Immunol* 2015; **6**: 623.
31. Muul LM, Tuschong LM, Soenen SL et al. Persistence and expression of the adenosine deaminase gene for 12 years and immune reaction to gene transfer components: long-term results of the first clinical gene therapy trial. *Blood* 2003; **101**: 2563–2569.
32. Di Ianni M, Falzetti F, Carotti A et al. Tregs prevent GVHD and promote immune reconstitution in HLA-haploidentical transplantation. *Blood* 2011; **117**: 3921–3928.
33. Brunstein CG, Miller JS, Cao Q et al. Infusion of ex vivo expanded T regulatory cells in adults transplanted with umbilical cord blood: safety profile and detection kinetics. *Blood* 2011; **117**: 1061–1070.
34. Brunstein CG, Miller JS, McKenna DH et al. Umbilical cord blood-derived T regulatory cells to prevent GVHD: kinetics, toxicity profile, and clinical effect. *Blood* 2016; **127**: 1044–1051.
35. Goettel JA, Biswas S, Lexmond WS et al. Fatal autoimmunity in mice reconstituted with human hematopoietic stem cells encoding defective FOXP3. *Blood* 2015; **125**: 3886–3895.
36. Moes N, Rieux-Laucat F, Begue B et al. Reduced expression of FOXP3 and regulatory T-cell function in severe forms of early-onset autoimmune enteropathy. *Gastroenterology* 2010; **139**: 770–778.
37. Abel S, Luckheide N, Westendorf AM et al. Strong impact of CD4<sup>+</sup> Foxp3<sup>+</sup> regulatory T cells and limited effect of T cell-derived IL-10 on pathogen clearance during *Plasmodium yoelii* infection. *J Immunol* 2012; **188**: 5467–5477.
38. Kurup SP, Obeng-Adjei N, Anthony SM et al. Regulatory T cells impede acute and long-term immunity to blood-stage malaria through CTLA-4. *Nat Med* 2017; **23**: 1220–1225.
39. Joshi NS, Akama-Garren EH, Lu Y et al. Regulatory T cells in tumor-associated tertiary lymphoid structures suppress anti-tumor T cell responses. *Immunity* 2015; **43**: 579–590.
40. Togashi Y, Shitara K, Nishikawa H. Regulatory T cells in cancer immunosuppression - implications for anticancer therapy. *Nat Rev Clin Oncol* 2019; **16**: 356–371.

## Supporting Information

Additional supporting information may be found online in the Supporting Information section at the end of the article.



This is an open access article under the terms of the Creative Commons Attribution-NonCommercial-NoDeriv License, which permits use and distribution in any medium, provided the original work is properly cited, the use is non-commercial and no modifications or adaptations are made.